Neotropical Ichthyology

Original article

https://doi.org/10.1590/1982-0224-2021-0040

Phylogeny of the Neotropical Pacman catfish genus *Lophiosilurus* (Siluriformes: Pseudopimelodidae)

Correspondence:
Oscar Akio Shibatta
shibatta@uel.br

Oscar A. Shibatta[1], Lucas R. Jarduli[1,2], Vitor P. Abrahão[3] and Lenice Souza-Shibatta[1]

Lophiosilurus is a monotypic genus represented by *L. alexandri*, a species endemic to the São Francisco river basin, Brazil. In previous phylogenetic analyses, the genus has been recovered as the sister group of *Cephalosilurus*. However, few species of *Cephalosilurus* or few characters were included in those studies. Thus, the current study aims to test the monophyletic hypothesis of the genera *Lophiosilurus* and *Cephalosilurus* with a more comprehensive phylogenetic analysis, including all *Cephalosilurus* species and a representative number of characters. Phylogenetic analyses of 18 terminal taxa (15 ingroups and three outgroups) were conducted based on a combined 75 character matrix, including 70 discrete morphological characters concerning osteology and neuroanatomy, four continuous characters, and the geometric morphometry of the head. The monophyly of the family Pseudopimelodidae was highly supported, and *Cephalosilurus* is synonymized with *Lophiosilurus*. The recovered phylogeny of the genus was (*L. albomarginatus* (*L. nigricaudus* (*L. apurensis* (*L. fowleri*, *L. alexandri*)))).

Keywords: Biodiversity, *Cephalosilurus*, Pacamã, Systematics, Taxonomy.

Submitted February 1, 2021
Accepted August 5, 2021
by Gloria Arratia
Epub December 10, 2021

1 Programa de Pós-Graduação em Ciências Biológicas, Departamento de Biologia Animal e Vegetal, Centro de Ciências Biológicas, Universidade Estadual de Londrina, 86057-970 Londrina, PR, Brazil. (OAS) shibatta@uel.br (corresponding author), (LSS) lenicesouza@hotmail.com.

2 Centro Universitário das Faculdades Integradas de Ourinhos, 19909-100 Ourinhos, SP, Brazil. (LRJ) lucasjarduli@gmail.com.

3 Programa de Pós-Graduação em Biodiversidade e Evolução, Instituto de Biologia, Universidade Federal da Bahia, Rua Barão de Geremoabo, 668, Ondina, 40170-115 Salvador, BA, Brazil. (VPA) vitorabrahao32@gmail.com.

Online version ISSN 1982-0224
Print version ISSN 1679-6225

Neotrop. Ichthyol.
vol. 19, no. 4, Maringá 2021

Lophiosilurus é um gênero monotípico representado por *L. alexandri*, uma espécie endêmica da bacia do rio São Francisco, Brasil. Em análises filogenéticas anteriores, o gênero foi recuperado como grupo irmão de *Cephalosilurus*. No entanto, poucas espécies de *Cephalosilurus* ou poucos caracteres foram incluídos nesses estudos. Assim, este estudo tem como objetivo testar a hipótese de monofilia dos gêneros *Lophiosilurus* e *Cephalosilurus*, com uma análise filogenética mais abrangente, incluindo todas as espécies de *Cephalosilurus* e um número representativo de caracteres. As análises filogenéticas de 18 táxons terminais (15 do grupo interno e três grupos externos) foram realizadas com base em uma matriz combinada de 75 caracteres, incluindo 70 caracteres morfológicos discretos de osteologia e neuroanatomia, quatro caracteres contínuos e um de morfometria geométrica da cabeça. A monofilia da família Pseudopimelodidae foi altamente apoiada e *Cephalosilurus* foi sinonimizado como *Lophiosilurus*. A filogenia recuperada do gênero foi (*L. albomarginatus* (*L. nigricaudus* (*L. apurensis* (*L. fowleri*, *L. alexandri*))).

Palavras-chave: Biodiversidade, *Cephalosilurus*, Pacamã, Sistemática, Taxonomia.

INTRODUCTION

Lophiosilurus Steindachner, 1876 is one of the seven genera of Pseudopimelodidae Fernández-Yépez, Antón, 1966, a catfish family endemic to South America, which comprises 53 valid species (Fricke *et al*., 2021). Although this is a small family in species number, it has a wide geographic distribution, occurring in drainages west of the Andes in Colombia and Ecuador, the Maracaibo basin, coastal rivers of Guianas and eastern Brazil, and the Orinoco, Amazonas, Araguaia-Tocantins, São Francisco, and La Plata (Paraná, Paraguay, Uruguay) river basins (Shibatta, 2003a; Shibatta, van der Sleen, 2018). Other genera of the family are *Pseudopimelodus* Bleeker, 1858, *Batrochoglanis* Gill, 1858, *Cephalosilurus* Haseman, 1911, *Microglanis* Eigenmann, 1912, *Cruciglanis* Ortega-Lara & Lehmann, 2006, and *Rhyacoglanis* Shibatta & Vari, 2017.

Lophiosilurus is a monotypic genus, represented by *L. alexandri* Steindachner, 1876, a species endemic to Brazil's São Francisco river basin. Its body morphology is the most differentiated within the family, especially concerning the broad and prognathous mouth, eye in dorsal position, low dorsal fin, small adipose fin, and depressed and wide-body (Assega *et al*., 2016). It has psammophilic behavior, burying itself and building nests in the sand. In addition, it feeds on fish, possesses a sit-and-wait strategy, and camouflage color from brown to greyish yellow. This fish has commercial value due to the consistency and flavor of its meat and has been the object of studies for cultivation in fish farming (*e.g*., Santos *et al*., 2013). In Brazil, it is popularly known as pacamão or pacamã, and internationally, among aquarists, as the Pacman catfish (Chang, 2013).

Phylogenetic analyses (*i.e*., Shibatta, 1998; Sullivan *et al*., 2013; Shibatta, Vari, 2017) have revealed *Lophiosilurus* as the sister group of *Cephalosilurus*. *Cephalosilurus* comprises *C. fowleri* Haseman, 1911 as type species, also endemic to the São Francisco river basin, *C. albomarginatus* (Eigenmann, 1912) from the Tukeit river basin, Guyana, *C. nigricaudus* (Mees, 1974) from the Sipaliwini river basin, Suriname, and *C. apurensis* (Mees, 1978)

from the Apure river basin, Venezuela, and Colombia (Fig. 1). *Cephalosilurus* is currently diagnosed by its prognathous mouth, color pattern with large dark brown blotches or spots, and depressed body slightly higher than *L. alexandri* (Shibatta, 1998). *Cephalosilurus fowleri* is also marketed as pacamã by professional fishers in the São Francisco river basin. However, the biology of this and other species of *Cephalosilurus* is poorly known.

In the last 20 years, knowledge of the systematics of Pseudopimelodidae has advanced considerably. Descriptions of new species and genera and new phylogenetic hypotheses have improved our understanding of the family (*e.g.*, Shibatta, 1998; Shibatta, Benine, 2005; Shibatta, Pavanelli, 2005; Ortega-Lara, Lehmann, 2006; Alcaraz *et al*., 2008; Jarduli, Shibatta, 2013; Shibatta, 2014; Shibatta, Vari, 2017; Shibatta, 2019). Morphological and molecular studies have established the monophyly of Pseudopimelodidae and its relationships within Pimelodoidea (*e.g.*, Lundberg *et al*., 1991a; Shibatta, 2003a; Diogo *et al*., 2004; Ortega-Lara, Lehmann, 2006; Birindelli, Shibatta, 2011; Sullivan *et al*., 2013; Shibatta, Vari, 2017; Abrahão *et al*., 2018). Although the monophyly of Pseudopimelodidae is strongly supported, the relationships among its members are only partially resolved. Although different studies have supported the close relationship between *Cephalosilurus*

FIGURE 1 | Geographic distribution of *Lophiosilurus* species. *Lophiosilurus apurensis*, MZUEL 6492, 189.7 mm SL, Apure river basin, Venezuela; *L. nigricaudus*, INPA 21632, 58.1 mm SL, Sipaliwini river basin, Suriname; *L. albomarginatus*, ROM 61336, 88.4 mm SL, Tukeit river basin, Guyana; *L. alexandri*, MZUEL 5377, 157.8 mm SL, São Francisco river basin, Brazil; *L. fowleri*, FMNH 54254, holotype, 301.4 mm SL, São Francisco river basin, Brazil.

and *Lophiosilurus* (*e.g.*, Shibatta, 2003b; Ortega-Lara, Lehmann, 2006; Birindelli, Shibatta, 2011; Sullivan *et al.*, 2013; Shibatta, Vari, 2017; Rangel-Medrano *et al.*, 2020; Silva *et al.*, 2021), they did not include all species in the clade (Fig. 2).

The depressed body is the most interesting feature shared by *Lophiosilurus* and *Cephalosilurus* that differentiate these genera from remaining pseudopimelodids. Body shape is often only indirectly included in phylogenetic analyses; however, new methods developed in the last two decades allow body shape to be incorporated with discrete and continuous morphological characters (Goloboff *et al.*, 2006; Catalano, Goloboff, 2018). Thus, studies combining different kinds of characters can improve the resolution and support in clades differentiable by body shape, refining our understanding of the evolution of studied groups (González-José *et al.*, 2008; Catalano *et al.*, 2015; Solis-Zurita *et al.*, 2019).

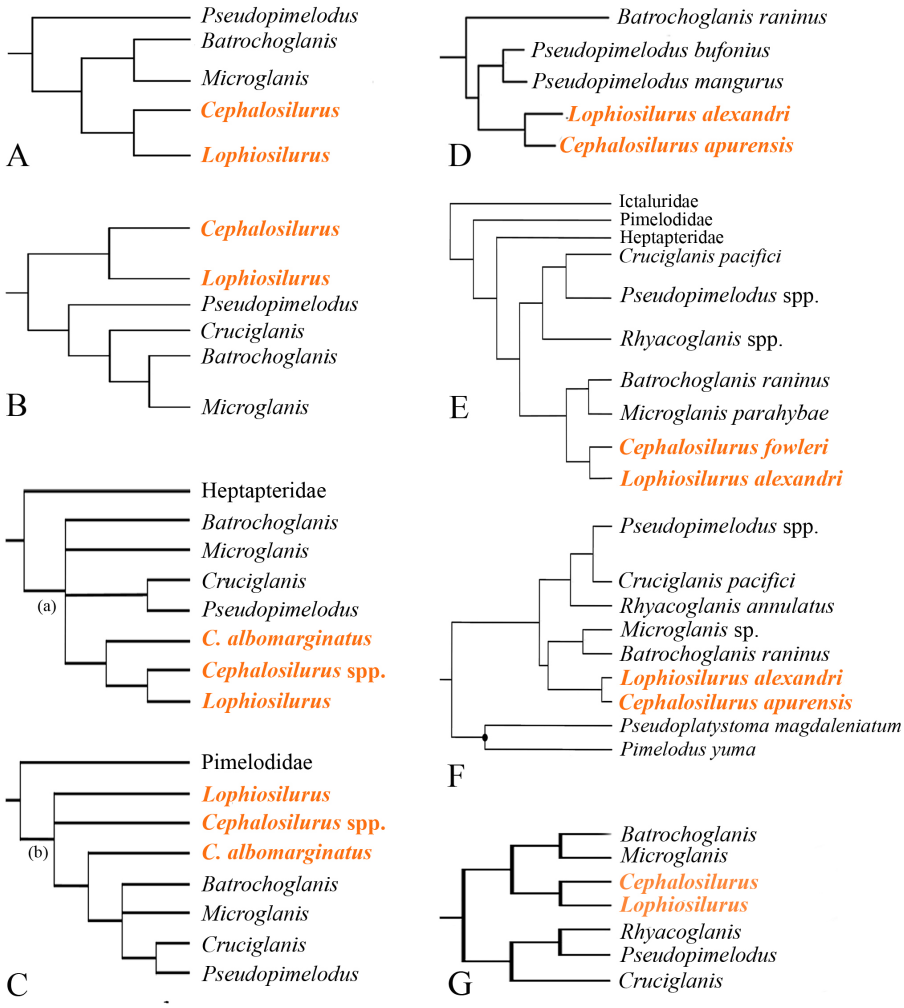

FIGURE 2 | Previous hypothesis of Pseudopimelodidae phylogeny: **A.** Shibatta (2003b); **B.** Ortega-Lara, Lehmann (2006); **C.** Birindelli, Shibatta (2011); **D.** Sullivan *et al.* (2013); **E.** Shibatta, Vari (2017); **F.** Rangel-Medrano *et al.* (2020); **G.** Silva *et al.* (2021).

In this contribution, we present a phylogenetic analysis, including all species of *Cephalosilurus* and *Lophiosilurus alexandri*, integrating discrete and continuous morphological characters derived from osteology, neuroanatomy, gas bladder morphology, morphometrics, counts, and head shape data. This study aims to test the hypothesis of *Cephalosilurus* monophyly and propose a new diagnosis for the group.

MATERIAL AND METHODS

Characters and taxa. The phylogenetic matrix included 75 morphological characters, 41 of them from Shibatta, Vari (2017), two from Ortega-Lara, Lehmann (2006), ten from Abrahão *et al*. (2018), and 22 new characters (17 discrete, four continuous, and one from geometric morphometry of head shape landmark configuration). The discrete characters were treated as non-additive, whereas continuous characters (*i.e*., coordinates of a landmark in space and measurements and counts after standardization) were analyzed in TNT as additive characters, using Farris optimization (Farris, 1970), with the implementation described in Goloboff *et al.* (2006) as applied in Ferrer *et al*. (2014). The continuous characters and counts were standardized (0–1; the maximum possible variation between any two taxa), with the implementation described in Goloboff *et al.* (2006). In this context, transformation costs are defined as the numerical difference between states. No discretization step (*e.g*., gap coding methods) is required.

The coding of character number four from Shibatta, Vari (2017) was changed for *Cruciglanis pacifici*, according to the original description (Ortega-Lara, Lehmann, 2006) and re-examination of the species. The analysis of the neurocranium of *Cruciglanis pacifici* is based on fig. 4a of Ortega-Lara, Lehmann (2006). Terminal taxa included twelve pseudopimelodid species analyzed by Shibatta, Vari (2017) plus three species of *Cephalosilurus* (*C. albomarginatus*, *C. apurensis*, and *C. nigricaudus*). *Ictalurus punctatus* (Rafinesque, 1818) (Ictaluridae), *Rhamdia quelen* (Quoy, Gaimard, 1824) (Heptapteridae), and *Steindachneridion scriptum* (Miranda Ribeiro, 1918) (Pimelodidae) were the outgroup taxa, with the former as the root of analysis. The results obtained herein indicate that *Cephalosilurus* is a junior synonym of *Lophiosilurus*. Following this, all species of *Cephalosilurus* will henceforth be treated as *Lophiosilurus*. Nomenclature of bones follows Arratia (2003a,b) and Birindelli (2014).

Examined material. The following specimens were used in this study (alc = alcohol; c&s = cleared and stained; gm = geometric morphometry): *Batrochoglanis raninus* (Valenciennes, 1840): MZUSP 23407 (2 c&s: not measured); INPA 1979 (1 alc/gm: 108.0 mm SL); INPA 7343 (1 alc/gm: 65.8 mm SL); INPA 8057 (1 alc/gm: 67.8 mm SL); INPA 19863 (2 alc/gm: 102.2–107.0 mm SL); INPA 34130 (3 alc/gm: 46.2–54.6 mm SL); LIRP 9435 (1 alc/gm: 51.8 mm SL); MZUEL 6035 (1 alc/gm: 77.6 mm SL). MZUSP 23407 (2 alc/gm: 50.7–74.4 mm SL); *Batrochoglanis villosus* (Eigenmann, 1912): ANSP 135903 (1 alc: 91.3 mm SL); MZUSP 7356 (2 c&s: not measured). *Cruciglanis pacifici* INCIVA (IMCN) 113 (1 alc/gm: 91.6 mm SL). *Ictalurus punctatus*: MZUEL 13834 (5 dry skel: not measured); MZUEL 6672 (10 alc/gm: 158.76–257.29 mm SL). *Lophiosilurus albomarginatus* (Eigenmann, 1912): ROM 61336 (17 alc/10 gm: 29.0–88.4 mm SL); FMNH 53221 (holotype: alc/gm: 75 mm SL); FMNH 53572 (paratype: alc/gm: 68.8 mm SL); FMNH 53222 (8 alc/gm: 21.5–58.5 mm SL); ROM 61482 (2 alc/gm: 50.5–78.8 mm SL). *Lophiosilurus alexandri*:

MZUEL 16469 (1 dry skel: not measured); MZUEL 5377 (3 alc/gm: 120.5–160.5 mm SL); MZUEL 13823 (1 alc/gm: 256.9 mm SL); MZUEL 16486 (1 alc/gm: 279.8 mm SL); MZUEL 19691 (2 alc/gm: 181.0–265.5 mm SL); MZUSP 96276 (1 alc/gm: 70.1 mm SL). *Lophiosilurus apurensis*: NRM 15995 (1 alc/gm: 201.9 mm SL); MZUEL 6492 (1 alc/gm: 186.0 mm SL); MZUEL 6493 (1 alc/gm: 188.4 mm SL); MZUSP 110996 (1 alc/gm: 180.3 mm SL); MZUSP 11099 (1 alc/gm: 200.2 mm SL). *Lophiosilurus fowleri* (Hasemann, 1911): ANSP 172158 (2 alc: 39.2–199.5 mm SL); FMNH 54254 (holotype: alc/gm: 301.4 mm SL); MCP 16675 (2 alc/gm: 44.9–128.0 mm SL); MCP 14094 (1 alc/gm: 328.8 mm SL); MCP 14126 (1 alc/gm: 262.7 mm SL); MZUSP 38097 (1 alc/gm: 244.6 mm SL); MZUSP 24647 (1 alc/gm: 277.0 mm SL). *Lophiosilurus nigricaudus* (Mees, 1974): INPA 21632 (2 alc/gm: 55.4–57.5 mm SL). *Microglanis parahybae* Steindachner, 1880: MNRJ 15989 (2 c&s: not measured; 5 alc/gm: 30.3–34.2 mm SL); MNRJ 16047 (5 alc.: 29.4–35.8 mm SL; 5 alc/gm: 28.6–38.9 mm SL). *Pseudopimelodus bufonius* (Valenciennes, 1840): MZUEL 5744 (20 alc/gm: 88.28–260.49 mm SL); MZUEL 07715 (1 alc/gm: 85.77 mm SL); INPA 8058 (1 alc/gm: 68.8 mm SL). *Pseudopimelodus mangurus* (Valenciennes, 1835): MZUEL 17690 (8 alc.: 112.0–190.4 mm SL); MZUEL 829 (1 alc/gm: 140.8 mm SL); MZUEL 1073 (1 alc/gm: 185.2 mm SL); MZUEL 3681 (1 alc/gm: 97.3 mm SL); MZUEL 6618 (1 alc/gm: 127 mm SL); MZUEL 1477 (2 alc/gm: 87.55–111.7 mm SL); MZUEL 1777 (1 alc/gm: 144, 53 mm SL); MZUEL 38278 (1 alc/gm: 83.55 mm SL); MZUEL 5741 (2 alc/gm: 159.9–208.2 mm SL); MCP 10336 (1 alc/gm: 129.0 mm SL); MCP 12685 (1 alc/gm: 146.1 mm SL); MCP 13087 (1 alc/gm: 173.7 mm SL). *Rhamdia quelen*: MZUEL 14631 (3 dry skel.: not measured); MZUEL 3845 (15 alc/gm: 104.6–193.3 mm). *Rhyacoglanis annulatus* Shibatta & Vari, 2017: ANSP 160625 (1 alc/gm: 42.5 mm SL); ANSP 192597 (1 alc/gm: 27.0 mm SL). *Rhyacoglanis epiblepsis* Shibatta & Vari, 2017: AMNH 40127 (25 paratypes alc/gm: 41.0–54.2 mm SL). *Rhyacoglanis paranensis* Shibatta & Vari, 2017: MZUEL 6034 (10 alc/gm: 44.6–38.7 mm SL); MZUEL 14121 (1 alc/gm: 89.3 mm SL); MZUEL 12159 (12 alc/gm: 33.7–27.6 mm SL). *Rhyacoglanis pulcher* Shibatta & Vari, 2017: BMNH 1880.12.8.105–107 (3 syntypes alc/gm: 58.5–68.5 mm SL). *Rhyacoglanis seminiger* Shibatta & Vari, 2017: LIRP 8042 (9 paratypes alc/gm: 48.3–74.8 mm SL); MZUEL 14123 (2 alc/gm: 60.4–64.8 mm SL); MZUSP 82085 (3 alc/gm: 44.4–70.4 mm SL). *Steindachneridion scriptum*: MZUEL 866 (1 c&s: 107.5 mm SL; 1 alc/gm: 602.2 mm SL); MZUEL 1482 (1 alc/gm: 163.3 mm SL); MZUEL 16238 (10 alc/gm: 101–125.9 mm SL). For additional material see Shibatta, Vari (2017) and Abrahão *et al*. (2018). Institutional abbreviations follow Sabaj (2019).

Geometric morphometry. Digital images of the head in the dorsal view of each specimen were taken with a 12.1 Mpixels High-Sensitivity CMOS sensor camera. Fourteen homologous landmarks (Fig. 3) were plotted in two dimensions using TPSDig 2.21 (Rohlf, 2015). The procedures performed to obtain the landmark data follow Catalano *et al.* (2015). First, all specimens of each species were superimposed using a General Procrustes Analysis (GPA; Gower, 1975; Rohlf, Slice, 1990) to obtain the consensus configurations representing each species shape. The consensus configurations derived from this step represent the shape of each species. Next, the TPSRelw 1.65 program (Rohlf, 2016) was used to obtain the GPA and consensus settings. The consensus configurations for each species were used to define multiple superimpositions using a new GPA. Finally, the multiple superimpositions were incorporated into a matrix of combined characters, generating a combined data set (see Tab. **S1**), as recommended by Catalano, Goloboff (2018).

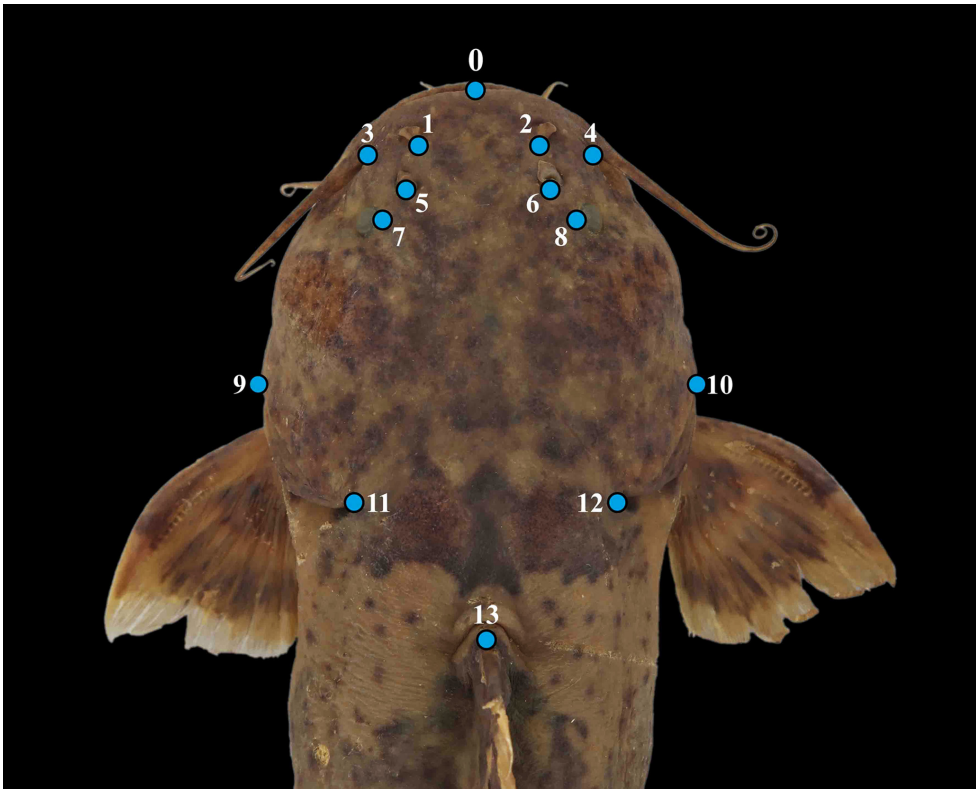

FIGURE 3 | Landmark position on *Pseudopimelodus mangurus*, MZUEL 1073, 185.2 mm SL. 0 = Tip of snout; 1 = Posterior margin of the left anterior nostril; 2= Posterior margin of the right anterior nostril; 3 = Insertion of left maxillary barbel; 4 = Insertion of right maxillary barbel; 5 = Posterior margin of the left posterior nostril; 6 = Posterior margin of the right posterior nostril; 7 = Medial margin of left eye; 8 = Medial margin of right eye; 9 = Most lateral point of the head in the left; 10 = Most lateral point of the head in the right; 11 = Upper end of the left operculum; 12 = Upper end of the right operculum; 13 = Insertion of dorsal fin spine.

Phylogenetic analysis. The combined matrix of discrete, continuous, and landmark data (see Tab. **S1**) was used to conduct the phylogenetic search under maximum parsimony in TNT program version 1.5 (Goloboff, Catalano, 2016; Catalano, Goloboff, 2018). The phylogenetic analysis was performed following the approach proposed by Catalano *et al.* (2010) to analyze landmark data. This approach maximizes the degree to which the similarity in landmark position in different taxa can be accounted for by common ancestry (Catalano, Goloboff, 2012). The tree score was given by the sum of the landmark displacements along the tree (Catalano *et al*., 2015). The tree score and ancestral shapes were established using the algorithms described in Goloboff, Catalano (2011) to optimize landmark data on a tree. This approach sets the optimal ancestral position of each landmark through a heuristic approximation, in which a grid is placed over the space occupied by all the observed locations for a given landmark. Each grid cell is considered a possible state (*i.e*., position) for the inner nodes. A cost matrix between states is constructed by calculating the distances between the centers of each of the cells. Once each of the observed positions has been assigned to the corresponding cell, the optimal positions are established using a cost matrix algorithm (Sankoff, Rousseau,

1975; Goloboff, 1998) to find the values for the ancestral nodes that minimize ancestor/descendant differences (Catalano *et al*., 2010). In this study, the landmark optimization was run with the following settings: 8×8 grid of cells; two levels of nested grids; observed landmark positions included as states and a final iterative improvement in the positions. The theoretical basis and algorithms for landmark analysis in a parsimony context are described in Catalano *et al.* (2010), Goloboff, Catalano (2011), Catalano, Goloboff (2012), and Goloboff, Catalano (2016).

The search strategy consisted of 5000 Random Addition Sequences (RAS = Wagner trees) followed by TBR (Tree Bisection and Reconnection algorithm) and holding 100 trees per replication. Branches supporting values were calculated using symmetric resampling (change probability set at 33%), with 5000 replications in TNT. Differential costs do not distort symmetric resampling, and the probability of increasing the weight of a character equals the probability of decreasing it (Goloboff *et al*., 2003; Goloboff *et al*., 2008). The retention index and the consistency index of the geometric morphometry character were computed according to Ospina-Garcés, Luna (2017).

RESULTS

Continuous characters description. The values of continuous characters 1 to 4 of each species are shown in Tab. **S2**.

1. Gill-rakers on first branchial arch; counts: minimum 2; maximum 27 (CI 0.84; RI 0.87). In *Ictalurus punctatus*, *Steindachneridion scriptum*, and *Rhamdia quelen*, the number of gill-rakers varies from 11 to 18 (median 15). In *Cruciglanis*, *Pseudopimelodus*, and *Rhyacoglanis*, the number is lower, ranging from 2 to 10 (median 6), as well as in *Batrochoglanis* and *Microglanis* from 6 to 11 (median 11). In *Lophiosilurus* species, the gill-rakers on the first branchial arch range from 9 to 27 (median 13.5), with the impressive highest number in *Lophiosilurus apurensis* with 27. Although most catfish species present less than 15 gill rakers on the first branchial arch, some Siluridae and Doradoidea present higher numbers (Birindelli, 2014). In Pseudopimelodidae, lower numbers of gill-rakers are shared by *Cruciglanis*, *Pseudopimelodus*, and *Rhyacoglanis* and are proposed as a synapomorphy for this group.

2. Dorsal-fin spine; length: minimum 5% of SL; maximum 21.3% of SL (CI 0.50; RI 0.10). In *Ictalurus punctatus*, *Rhamdia quelen*, and *Steindachneridion scriptum*, the ossified portion of the dorsal-fin spine is elongated, with size ranging from 8.2 to 16.2% of SL. The dorsal-fin spine of Pseudopimelodidae is usually longer, varying between 8.7 to 21.3% of SL. However, in *Lophiosilurus alexandri*, the dorsal-fin spine is extremely short, with the dorsal-fin spine length varying from 5 to 5.9% of SL.

3. Body depth relative to body width; distance between pectoral girdles: minimum 33.2%; maximum 116.6% (CI 0.45; RI 0.43). The body of *Rhamdia quelen* (101.4%) and *Ictalurus punctatus* (111.6–116.6%) is the deepest among the examined material. The body is slightly shallower in *Steindachneridion scriptum*, *Cruciglanis pacifici*, *Microglanis parahybae*, *Pseudopimelodus*, and *Rhyacoglanis* (ranging from 61% to 92.9%). *Lophiosilurus albomarginatus*, *L. apurensis*, *L. fowleri*, and *Batrochoglanis raninus* exhibit body depth proportions from 58.6 to 67.7%. *Lophiosilurus alexandri* and *L. nigricauda* are the most depressed, with body widths of 33.2–47.8% and 48.7%, respectively. Assega *et*

al. (2016) observed negative allometry in the body depth of *L. alexandri* throughout its development and discussed the phylogenetic meaning of body depth. According to those authors, a relatively deep body is plesiomorphic, and a depressed body is apomorphic.

4. Adipose-fin base; length: minimum 4.6% of SL; maximum 43.4% of SL (CI 0.54; RI 0.04). The most extended adipose-fin base length is observed in *Rhamdia quelen* (37–43.5%), and the shortest is observed in *Lophiosilurus alexandri* (4.6–7.44%). Most Pseudopimelodidae, *Ictalurus punctatus*, and *Steindachneridion scriptum* have intermediate values. A large adipose fin base is present in *Dyplomystes nahuelbutaensis* since small juveniles (Lundberg *et al*., 2004), corroborating the plesiomorphic condition of character in Siluriformes.

Discrete characters description.

Skin and dermal structures. Characters 5 to 8 herein are described as 1 to 4 in Shibatta, Vari (2017).

5. Unculiferous tubercles; (0) absent; (1) present (Shibatta, Vari, 2017: fig. 14) (CI 1.00; RI 1.00).

6. Unculiferous epidermal structures; degree of development: (0) little developed; (1) well developed (CI 0.33; RI 0.60).

7. Skin covering pectoral-fin spine; thickness: (0) thin; (1) thick (CI 0.33; RI 0.71).

8. Axillary pore: (0) present; (1) absent (CI 0.50; RI 0.50).

Pigmentation. Characters 9 to 17 herein are described as 5 to 13 in Shibatta, Vari (2017).

9. Light blotch on the cheek: (0) absent; (1) present (CI 1.00; RI 1.00).

10. Dark brown mask well defined on the head: (0) absent; (1) present (CI 1.00; RI 1.00).

11. Dark band on predorsal region: (0) absent; (1) present (CI 0.33; RI 0.60).

12. Fusion of dark predorsal and subdorsal bands: (0) absent (1) partial, (2) complete (CI 1.00; RI 1.00).

13. Dark bands on the trunk and caudal peduncle: (0) absent throughout ontogeny; (1) present at some point during ontogeny (CI 1.00; RI 1.00).

14. Fusion of dark subdorsal and subadipose bands: (0) absent; (1) present (CI 0.33; RI 0.00).

15. Small scattered spots on the lateral surface of the body: (0) limited in number, widely dispersed; (1) numerous, closely dispersed (CI 0.33; RI 0.00).

16. Dark caudal-fin stripe: (0) absent; (1) present (CI 0.50; RI 0.80).

17. Caudal fin; pigmentation: (0) middle of the dark caudal-fin stripe without convergence with dark caudal-peduncle band; (1) middle stripe convergent with caudal-peduncle band; (2) entire fin dark (CI 1.00; RI 1.00).

18. Caudal fin dark-spot; configuration (char. 61 from Ortega-Lara, Lehman, 2006): (0) without dark spot; (1) with a dark spot at its base and fused with the peduncular spot, covering the anterior three-quarters of its length, and distal rim hyaline. (CI 0.33; RI –). Among species analyzed, state 1 is shared by *Cruciglanis pacifici* (Ortega-Lara, Lehmann, 2006: fig. 5), *Lophiosilurus albomarginatus*, and *L. nigricaudus*.

Jaws. Characters 19 to 20 herein are described as 13 to 14 in Shibatta, Vari (2017).

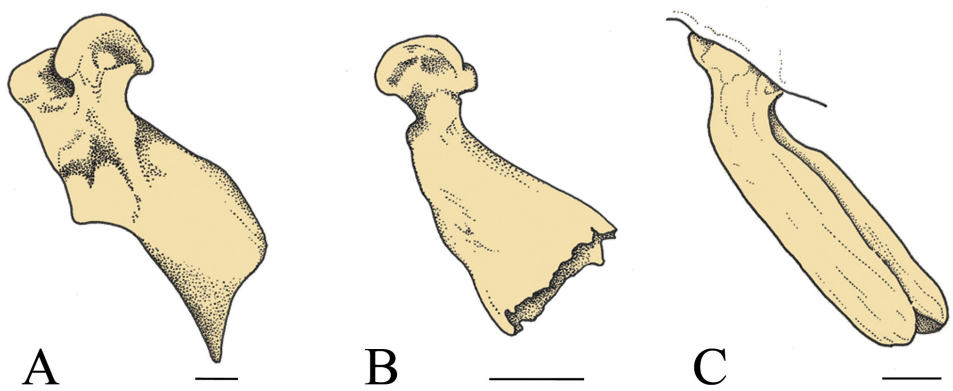

FIGURE 4 | Dorsal view of left maxillary bone; anterior up: **A.** *Steindachneridion scriptum*, MZUEL 19302; **B.** *Rhamdia quelen*, MZUEL 14631; **C.** *Lophiosilurus apurensis*, MBUCV-V-15379. Scale bars = 1 mm.

19. Premaxilla; bifurcated dorsolateral process:(0) absent; (1) present (autapomorphy).

20. Premaxillary tooth plate; form: (0) not posterolaterally extended; (1) posterolaterally extended (autapomorphy).

21. Posterior portion of maxillary bone; shape: (0) pointed; (1) irregular; (2) rounded (Fig. 4) (CI 1.00; RI 1.00). In *Ictalurus punctatus* and *Steindachneridion scriptum*, the posterior extremity of maxillary bone is pointed (state 0), and in *Rhamdia quelen*, it is irregular (state 1). In almost all species of Pseudopimelodidae, the maxillary bone can be posteriorly pointed (state 0). However, in *Lophiosilurus albomarginatus*, *L. alexandri*, *L. apurensis*, and *L. fowleri*, the maxillary bone is posteriorly semi-circular (state 2).

Head and neurocranium. Characters 22 to 25 herein are described as 15 to 18 in Shibatta, Vari (2017).

22. Anterior nostril; location: (0) distant from the margin of mouth; (1) near the margin of mouth (CI 1.00; RI 1.00).

23. Vomer: (0) present; (1) absent (Ortega-Lara, Lehmann, 2006: fig. 3) (CI 1.00; RI 1.00).

24. Lateral ethmoid-autopalatine joint; length: (0) abridged, autopalatine only touching the lateral ethmoid (Shibatta, 2019: fig. 2); (1) elongated, about 1/6 of autopalatine articulated with lateral ethmoid (autapomorphy).

25. Autopalatine; shape: (0) depth similar anteriorly and posteriorly; (1) depth greater posteriorly; spoon-shaped (Shibatta, 2019: fig. 3) (CI 1.00; RI 1.00).

26. Medial constriction on mesethmoid: (0) present; (1) absent (Fig. 5) (CI 1.00; RI 1.00). In *Ictalurus punctatus*, *Rhamdia quelen*, and *Steindachneridion scriptum*, the mesethmoid has a constriction, widening posteriorly (state 0). This plesiomorphic condition is also observed in *Lophiosilurus albomarginatus*, *Batrochoglanis raninus*, *Microglanis parahybae*, *Pseudopimelodus mangurus*, *Rhyacoglanis paranensis*, *R. epiblepsis*, and *Cruciglanis pacifici*. However, in *L. alexandri*, *L. apurensis*, and *L. fowleri*, constriction does not occur, and the mesethmoid is nearly trapezoidal, wider anteriorly than posteriorly (state 2).

27. Anterior frontal fontanel; shape: (0) as a groove (1) ellipsoid (Fig. 5) (CI 0.50; RI 0.50). In *Ictalurus punctatus*, *Rhamdia quelen*, and *Steindachneridion scriptum*, the anterior frontal fontanel is narrow and long as a groove (state 0) as in many Pseudopimelodidae. However, in *Batrochoglanis raninus*, *Microglanis parahybae*, and *Lophiosilurus albomarginatus*, it is wide with an ellipsoid shape (state 1).

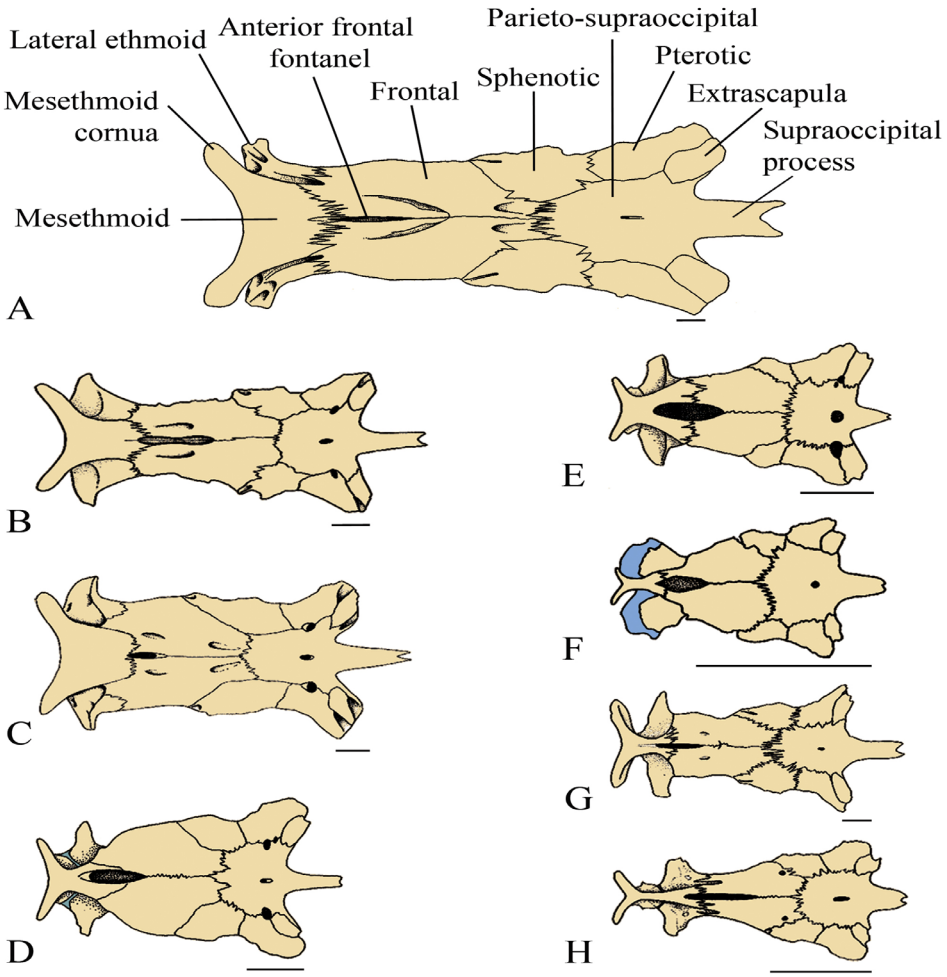

FIGURE 5 | Neurocranium in dorsal view: **A.** *Lophiosilurus alexandri*, MZUEL 5542; **B.** *L. fowleri*, MZUEL 12095; **C.** *L. apurensis*, MBUCV-V-15379; **D.** *L. albomarginatus*, ROM 61336; **E.** *Batrochoglanis raninus*, MZUSP 23407; **F.** *Microglanis parahybae*, MNRJ 15989; **G.** *Pseudopimelodus mangurus*, MZUEL 12937; **H.** *Rhyacoglanis paranensis*, MZUEL 6034. Bones in yellow and cartilage in bluish grey. Scale bars = 5 mm.

28. Orbitosphenoid flap-like projection: (0) absent; (1) present (CI 0.50; RI –). In *Ictalurus punctatus* and *Rhamdia quelen*, the orbitosphenoid does not has a ventral flap-like projection. Nevertheless, it is present in *Steindachneridion scriptum* and all species of Pseudopimelodidae.

29. Orbitosphenoid flap-like projection; anterior width: (0) narrower than parasphenoid width; (1) similar to parasphenoid width; (2) broader than parasphenoid width (CI 0.66; RI 0.66). In *Lophiosilurus alexandri*, *L. fowleri*, and *Batrochoglanis raninus*, the orbitosphenoid is narrower than parasphenoid (state 0). The orbitosphenoid and parasphenoid widths are similar in *Steindachneridion scriptum* and *Pseudopimelodus mangurus* (state 1). In *Microglanis parahybae* and *Rhyacoglanis epiblepsis*, and *R. paranaensis*, the width is more extensive (state 2). This character is inapplicable in *Ictalurus punctatus* and *Rhamdia quelen* since the orbitosphenoid does not have a lateral flap-like projection in the ventral region of the neurocranium lateral to the parasphenoid.

30. Frontal; shape: (0) trapezoidal with wide anterior; (1) trapezoidal with broad posterior; (2) rectangular (Fig. 5) (CI 0.67; RI 0.67). In Siluriformes, the shape of the frontal bone is quite variable. In *Ictalurus punctatus*, the frontal bone has a greater width in the anterior region, at the lateral ethmoid level, than in the posterior region at sphenotic level (state 0). In *Rhamdia quelen*, *Steindachneridion scriptum*, *Batrochoglanis raninus*, *Microglanis parahybae*, *Lophiosilurus albomarginatus*, *Rhyacoglanis paranensis*, and *R. epiblepsis*, the posterior region is wider than the anterior one (state 1). The width of the anterior frontal area in *Pseudopimelodus mangurus*, *Lophiosilurus alexandri*, *L. fowleri*, and *L. apurensis* is similar to that of the posterior region (state 2).

31. Anterior frontal fontanel; configuration (char. 59 from Ortega-Lara, Lehman, 2006): (0) not reaching posteriorly to the level of the infraorbital sensory canal opening of the sphenotic bone; (1) reaching that level. (CI 0.50; RI 0.67). In *Ictalurus punctatus*, *Rhamdia quelen*, *Steindachneridion scriptum*, and *Cruciglanis pacifici*, the anterior frontal fontanel reaches the level of the infraorbital canal opening of the sphenotic bone (state 0). In other analyzed species of Pseudopimelodidae, the anterior frontal fontanel is shorter (state 1) (Fig. 5; Ortega-Lara, Lehmann, 2006: fig. 4).

32. Parietal-supraoccipital; shape: (0) trapezoidal; (1) square (Fig. 5) (CI 0.25; RI 0.40). In *Ictalurus punctatus* and *Rhamdia quelen*, the parietal-supraoccipital is trapezoidal and wider posteriorly (state 0). Species of *Lophiosilurus* and *Pseudopimelodus mangurus* exhibit this same condition. A quadrangular form without posterior expansion occurs in *Steindachneridion scriptum*, *Batrochoglanis raninus*, *Microglanis parahybae*, *Cruciglanis pacifici*, and *Rhyacoglanis epiblepsis* (state 1).

33. Infraorbitals; shape: (0) gradually expanding posteriorly; (1) wide uniformly (Shibatta, 2019: fig. 2) (CI 0.50; RI 0.67). In *Ictalurus punctatus*, *Rhamdia quelen*, *Steindachneridion scriptum*, and *Lophiosilurus alexandri*, the infra-orbital bones gradually expand posteriorly (state 0). The width is consistent from second to fifth (state 1) in all other pseudopimelodids.

34. Ectopterygoid: (0) present; (1) absent (CI 1.00; RI –). The ectopterygoid is present and homologous across most Siluriformes groups, and this condition is observed in *Steindachneridion scriptum* and all species of Pseudopimelodidae examined herein (state 0). However, in *Rhamdia quelen*, this bone is absent (state 1).

35. Ectopterygoid posterior prolongation; medial shape: (0) straight; (1) concave; (2) convex (Fig. 6) (CI 0.60, RI 0.33). In *Steindachneridion scriptum*, the medial region of posterior prolongation of the ectopterygoid is straight (state 0). This character is inapplicable in *Ictalurus punctatus* and *Rhamdia quelen* by the absence of ectopterygoid. Also, in *Lophiosilurus albomarginatus* and *L. apurensis*, the ectopterygoid is present, but the prolongation is absent and coded as inapplicable. In *Batrochoglanis raninus*, *Lophiosilurus alexandri*, *L. fowleri*, *Microglanis parahybae*, *Pseudopimelodus mangurus*, *Rhyacoglanis paranensis*, and *R. epiblepsis*, the prolongation is concave (state 1). In *Cruciglanis pacifici*, it is convex (state 2).

36. Anterior portion of entopterygoid; shape: (0) approximately straight; (1) narrowing anteriorly to rounded tip (Fig. 6) (CI 1.00, RI 1.00). The entopterygoid has the anterior region almost straight and broad as the posterior one in *Steindachneridion scriptum* and *Rhamdia quelen* (state 0). In Pseudopimelodidae, there is a tip in the anterior region (state 1).

37. Posterior portion of entopterygoid; shape: (0) almost straight, without posterior

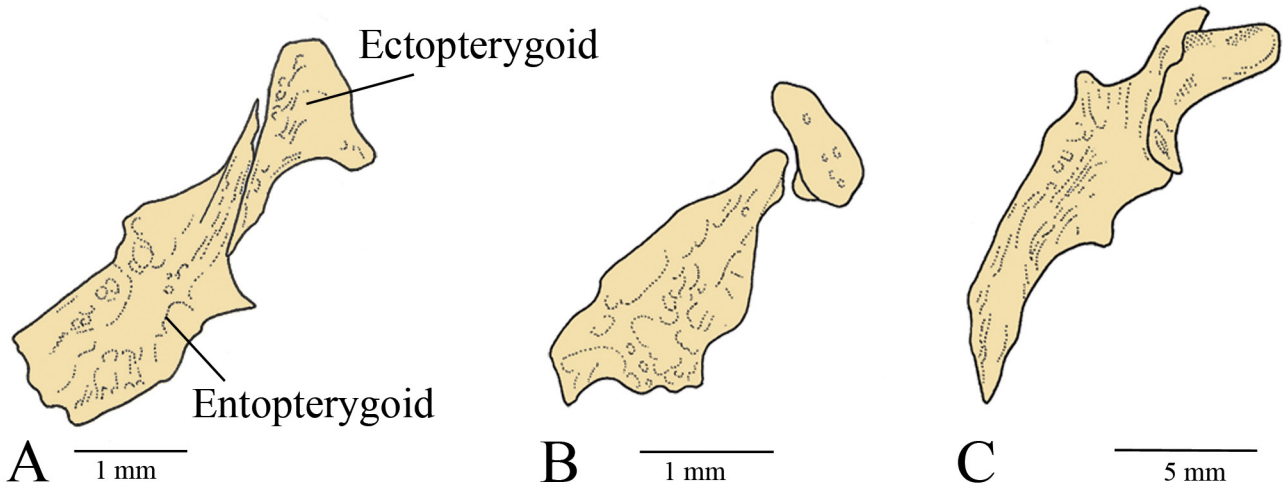

FIGURE 6 | Ventral view of left ectopterygoid and entopterygoid bones; anterior up: **A.** *Batrochoglanis raninus*, MZUSP 23407; **B.** *Lophiosilurus albomarginatus*, ROM 61336; **C.** *Lophiosilurus alexandri*, MZUEL 5542.

projection; (1) with a posterior projection; (2) sharp tip (Fig. 6) (CI 0.67, RI 0.67). In *Steindachneridion scriptum*, *Rhamdia quelen*, *Batrochoglanis raninus*, *Microglanis parahybae*, *Pseudopimelodus mangurus*, *Rhyacoglanis paranensis*, and *R. epiblepsis*, the posterior region of the entopterygoid has a relatively uniform width along its length and a truncated posterior portion without projection (state 0). This structure ends in a small projection in *Cruciglanis pacifici*, *Lophiosilurus albomarginatus*, and *L. apurensis* (stage 1). In *Lophiosilurus alexandri* and *L. fowleri*, the entopterygoid has a prolonged sharp tip in the posterior region (state 2).

Hyoid and gill arches. Characters 38 to 42 herein are described as 19 to 23 in Shibatta, Vari (2017).

38. Dorsal hypohyal: (0) present; (1) absent (Shibatta, 2019: fig. 6) (CI 1.00; RI 1.00).

39. Second basibranchial; shape: (0) without lateral processes; (1) with lateral processes resulting in a cruciform shape (Ortega-Lara, Lehmann, 2006: fig. 2) (autapomorphy).

40. Metapterygoid; shape: (0) longer than wide; (1) as long as wide (Lundberg *et al.* 1991a: fig. 9) (CI 1.00; RI 1.00).

41. Fenestra in quadrate: (0) absent; (1) present (Shibatta, 2019: fig. 5) (CI 1.00; RI 1.00).

42. Gill rakers on first branchial arch; distribution: (0) along the anterior margin of ceratobranchial; (1) restricted to the posterior region of anterior margin of ceratobranchial (Shibatta, 2019: fig. 7) (CI 0.33; RI 0.60).

43. Gill rakers on first branchial arch; shape: (0) conical and elongated, without bifurcation; (1) bifurcated or even branched (Fig. 7) (CI 1.00; RI 1.00). In most species of Pseudopimelodidae, in *Ictalurus punctatus*, *Rhamdia quelen*, and *Steindachneridion scriptum*, the gill rakers are elongated and not bifurcated (state 0). Bifurcated gill rakers are found only in *Lophiosilurus albomarginatus*, *L. alexandri*, *L. apurensis*, and *L. fowleri* within Pseudopimelodidae (state 1).

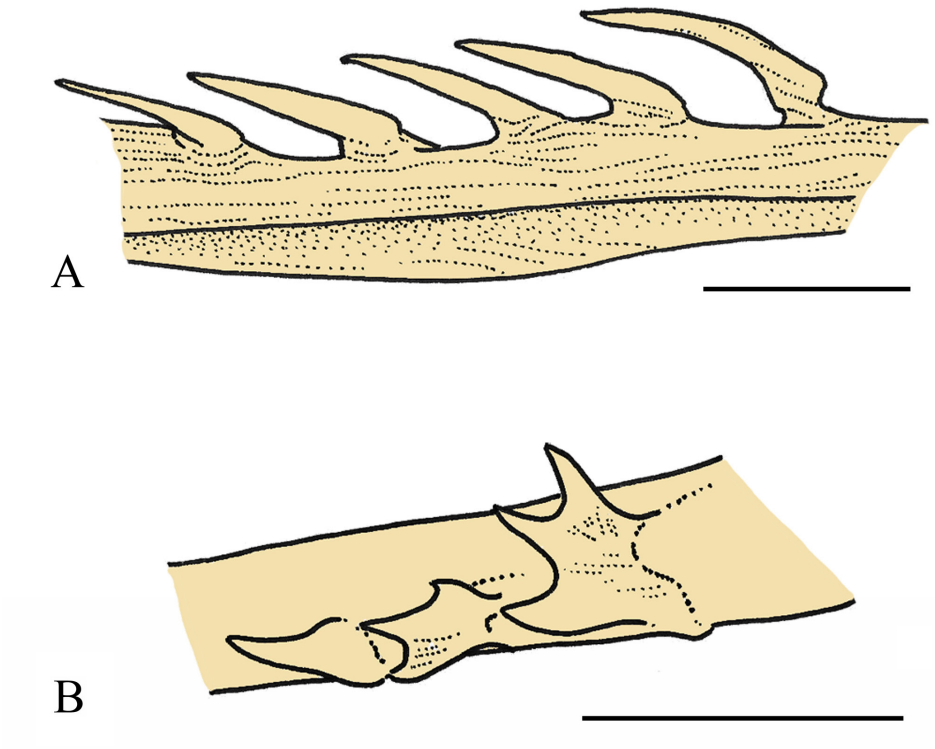

FIGURE 7 | Shape of gill rakers on the first ceratobranchial; lateral view of left selected portion; anterior to left: **A.** *Steindachneridion scriptum*, MZUEL 19302; **B.** *Lophiosilurus alexandri*, MZUEL 5542. Scale bars = 5 mm.

Appendicular and axial skeleton. Characters 44 to 49 and 51 to 55 herein are described as 24 to 34 in Shibatta, Vari (2017).

44. Mesocoracoid arch; shape: (0) elongate (Shibatta, 2019: fig. 8); (1) triangular (CI 1.00; RI 1.00).

45. Posterior cleithral process; length: (0) elongate, more than half continuing posteriorly to the margin of opercular membrane; (1) short, broadly covered by an opercular membrane (CI 0.50; RI 0.80).

46. Branched pectoral-fin rays; number: (0) 8 or more; (1) 7; (2) 6; (3) 5 (CI 0.75; RI 0.80).

47. Serrae along anterior and posterior margins of pectoral-fin spine; height: (0) shorter anteriorly; (1) all of the same approximate length (CI 0.40; RI 0.50).

48. Serrae along the anterior margin of pectoral-fin spine; distribution: (0) across entire margin; (1) restricted to base (CI 0.50; RI 0.00).

49. Tip of pectoral-fin spine; shape: (0) pointed; (1) bifurcated (CI 0.33; RI 0.67).

50. Anterior process of parapophysis of the fourth vertebra; shape: (0) straight, not curved; (1) ventrally curved; (2) laterally swelled (Fig. 8) (CI 1.00; RI 1.00). In *Ictalurus punctatus*, the anterior transverse process of the fourth vertebra is almost entirely straight, as is *Steindachneridion scriptum* and *Rhamdia quelen* (state 0). This vertebra is ventrally curved in *Pseudopimelodus mangurus* and *Rhyacoglanis paranensis*, forming a folding structure (state 1). In *Lophiosilurus*, *Batrochoglanis raninus*, and *Microglanis parahybae*, only the lateral tip is swelled (state 2).

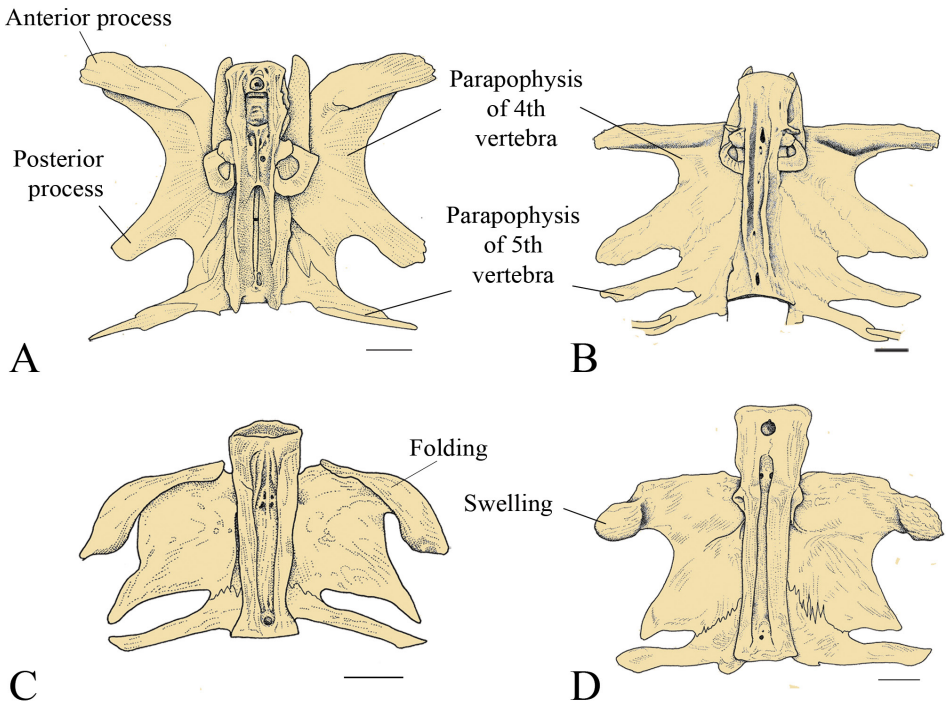

FIGURE 8 | Ventral view of complex vertebrae; anterior up: **A.** *Ictalurus punctatus*, MZUEL 13834; **B.** *Steindachneridion scriptum*, MZUEL, 19302; **C.** *Pseudopimelodus mangurus*, MZUEL 17286; **D.** *Lophiosilurus alexandri*, MZUEL 5542. Scale bar = 5 mm.

51. Fifth and sixth centra; joint: (0) not interdigitating; (1) deeply interdigitating (Lundberg *et al*., 1991b: fig. 12) (autapomorphy).

52. Vertebrae; number: (0) 46 or more; (1) 36–45; (2) 30–35 (CI 0.50; RI 0.71).

53. Dorsal-fin spine; serration: (0) smooth anteriorly; (1) serrated anteriorly (CI 0.33; RI 0.71).

54. Caudal fin; shape: (0) two pointed lobes; (1) two rounded lobes; (2) two subtle rounded lobes (emarginated); (3) no distinct lobes (rounded) (CI 0.60; RI 0.71).

55. Caudal-fin lobes; length: (0) lobes approximately equal; (1) ventral lobe longer; (2) dorsal lobe longer (CI 0.40; RI 0.67).

56. Dorsal lobe of the caudal skeleton; composition: (0) hypurals 3, 4, and 5 free; (1) hypural 5 free, hypurals 3 and 4 fused; (2) hypurals 3, 4, 5 fused (Fig. 9) (CI 0.67; RI –). In *Ictalurus punctatus* and *Steindachneridion scriptum*, the caudal bones have hypurals 3, 4, and 5 free (state 0). State 1 is observed in *Rhamdia quelen*, *Pseudopimelodus mangurus*, *Batrochoglanis raninus*, *Microglanis parahybae*, *Lophiosilurus apurensis*, and *L. fowleri*. State 2 occurs in *L. alexandri*.

57. Ventral lobe of caudal skeleton; composition: (0) parhypural and hypural 1 free; (1) parhypural and hypural 1 fused (Fig. 9) (CI 1.00; RI 1.00). In *Ictalurus punctatus*, *Rhamdia quelen*, and *Steindachneridion scriptum*, all elements of ventral caudal bones are free (state 0). Conversely, state 1 is observed in all examined species of Pseudopimelodidae.

Gas bladder. Characters 58 to 61 herein are described as 35 to 38 in Shibatta, Vari (2017).

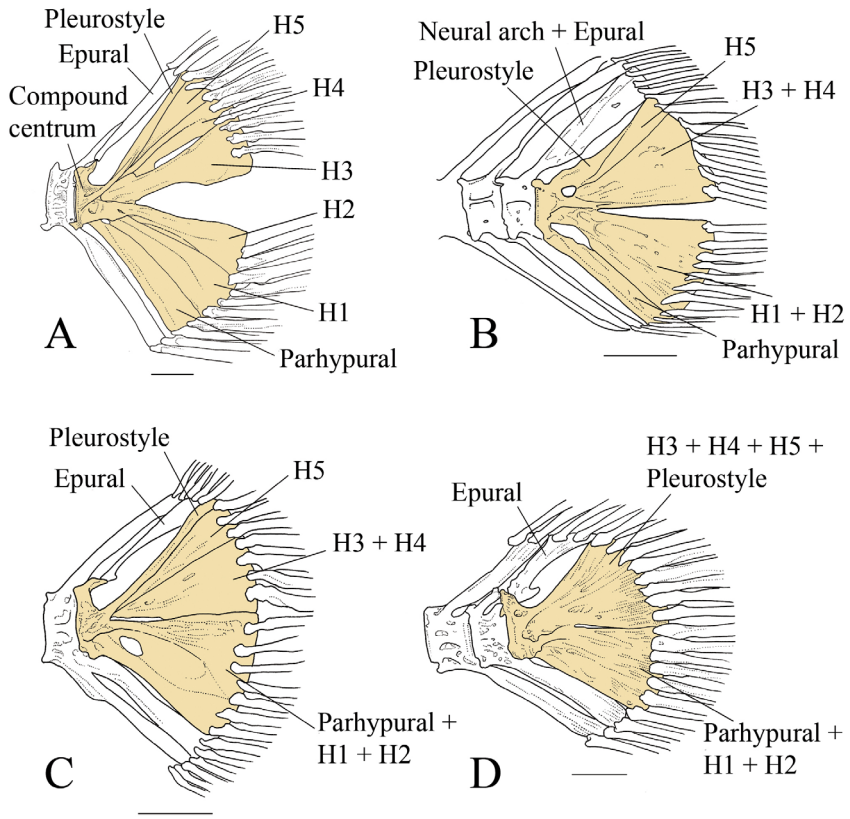

FIGURE 9 | Lateral view of caudal bones; anterior to left: **A.** *Steindachneridion scriptum*, MZUEL 19302; **B.** *Rhamdia quelen*, MZUEL 11664; **C.** *Pseudopimelodus mangurus*, MZUEL 17286; **D.** *Lophiosilurus alexandri*, MZUEL 13288. Scale bars = 5 mm.

58. Gas bladder; shape: (0) heart-shaped; (1) dumbbell-shaped (Birindelli, Shibatta, 2011: fig. 1) (CI 1.00; RI 1.00).

59. Constrictor muscle of gas bladder; presence: (0) absent; (1) present (CI 0.50; RI 0.67)

60. Lateral trabeculae on internal T-shaped gas bladder septum; presence: (0) absent; (1) present (CI 0.50; RI 0.80).

61. Pseudotympanum opening; size: (0) large, height about twice the diameter of the eye; (1) small, height approximately equal to the diameter of the eye (Birindelli, Shibatta, 2011: fig. 2) (CI 0.50; RI 0.83).

Laterosensory system and maxillary barbel. Characters 62 to 64 herein are described as 39 to 41 in Shibatta, Vari (2017).

62. Lateral line; length: (0) complete; (1) incomplete but long; extending beyond vertical through adipose fin; (2) incomplete and short; falling short of vertical through adipose fin (Ruiz, Shibatta, 2010: fig. 3) (CI 0.40; RI 0.00).

63. Cephalic lateral line; arrangement: (0) unbranched (Shibatta, 2019: fig. 14); (1) branched (Lundberg *et al*., 1991b: fig. 11) (autapomorphy).

64. Maxillary barbel; length: (0) long; extending beyond vertical through the dorsal-fin origin; (1) short; falling short of vertical through the dorsal-fin origin (CI 1.00; RI 1.00).

Gross brain morphology. The following characters (65 to 74) were obtained from Abrahão *et al.* (2018; corresponding numbers in parenthesis) and renumbered here; a detailed discussion on each character can be obtained from that paper. In addition, Abrahão *et al*. (2018) generalized character states for family or genus after examining several of their representatives. The same was followed in this work.

65. Intumescence on *lobus facialis*, position (char. 1): (0) oriented along the entire lateral margin of each lobe; (1) located along the anterolateral portion; (2) anteriorly placed (Fig. 10) (CI 100; RI 100). In Ictaluridae and Heptapteridae, the *lobus facialis* appears to have two regions longitudinally subdivided into two halves (state 0). Pimelodidae, *Pseudopimelodus*, *Microglanis*, *Batrochoglanis*, *Cruciglanis*, and *Rhyacoglanis* the lobus facialis anterolaterally, occupying half the width of each lobe in the posterior portion and extending to the anteromedial part (state 1). In *Lophiosilurus*, the intumescence on *lobus facialis* is anteriorly placed (state 2).

66. Posterior portion of the lateral line lobe; configuration (char. 2): (0) reaching the half-length of the *lobus facialis*; (1) reaching the anterior part of the *lobus vagi* (Fig. 10) (CI 100; RI 100). In Ictaluridae and Heptapteridae, the prolongation of the posterior portion of the lateral-line lobe ends abruptly and reaches only half the length of the lateral margin of lobus facialis (state 0). In Pimelodidae and Pseudopimelodidae, the posterior portion of the lateral-line lobe has a tail-shaped prolongation that extends beyond the division between *lobus facialis* and *lobus vagi* (state 1).

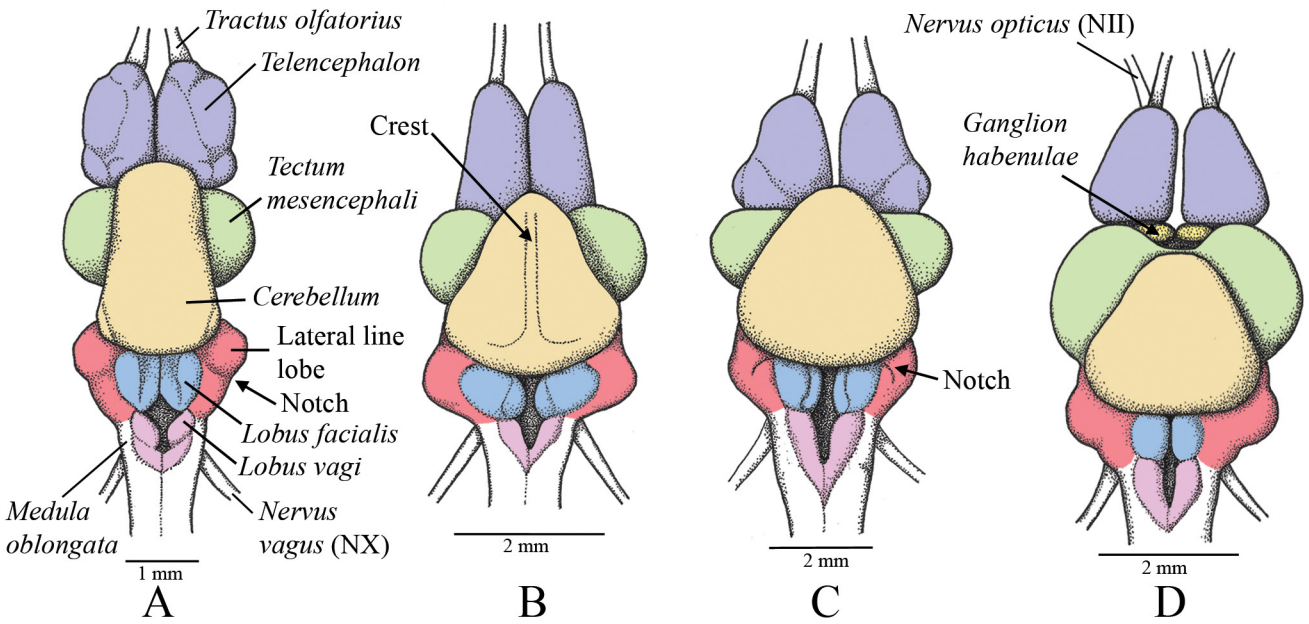

FIGURE 10 | Dorsal view of brain; anterior up: **A.** *Rhamdia quelen*, MZUEL 6036, 222.4 mm SL; **B.** *Rhyacoglanis paranensis*, MZUEL 6034, 39.2 mm SL; **C.** *Cruciglanis pacifici*, MCP non-catalogued, 142.4 mm SL; **D.** *Lophiosilurus alexandri*, MZUEL 5377, 58.7 mm SL.

67. *Saccus vasculosus*; relative size (char. 3): (0) smaller than the pituitary gland; (1) same size or larger than the pituitary gland (CI 1.00; RI 1.00). In Ictaluridae and Heptapteridae, saccus vasculosus is smaller than the pituitary gland. On the other hand, the saccus vasculosus is more conspicuous in Pimelodidae and Pseudopimelodidae, with the same size or larger than the pituitary gland (state 1).

68. Conspicuous bulge on the anterior portion of *lobus vagi* (char. 4): (0) present; (1) absent (Fig. 10) (CI 1.00; RI 1.00). In Ictaluridae, Heptapteridae, and Pimelodidae, there is a prominent bulge on the anterior portion of the lobus vagi (state 0). In all examined Pseudopimelodidae, such bulge is less conspicuous or absent (state 1).

69. *Cerebellum*; general shape (char. 5): (0) oval-shaped; (1) somewhat triangular (Fig. 10). (CI 1.00; RI 1.00). In Ictaluridae, Heptapteridae, and Pimelodidae, the *cerebellum* has an oval shape with the posterior region rounded (state 0). The same condition is observed in *Pseudopimelodus*, *Cruciglanis*, and *Rhyacoglanis*. In *Batrochoglanis*, *Microglanis*, *Cephalosilurus*, and *Lophiosilurus*, the cerebellum is somewhat triangular with the posterior margin straight, and an anterior margin rounded or at an acute angle (state 1).

70. Anterior portion of the *cerebellum*; prolongation (char. 6): (0) extending beyond the half-length of the *telencephalon*; (1) extends until the posterior portion of *telencephalon*; (2) extends as far as boundary between *mesencephalon* and *telencephalon* (also exhibiting *habenula* in the dorsal portion of the *diencephalon*) (Fig. 10) (CI 1.00; RI 1.00). In Ictaluridae, Heptapteridae, and Pimelodidae, the *cerebellum* is longer, with its anterior portion prolonged beyond the half-length of the *telencephalon* (state 0). In *Pseudopimelodus*, *Cruciglanis*, and *Rhyacoglanis*, the *cerebellum* has intermediate size, with the anterior portion reaching until the *telencephalon's* posterior portion (state 1). In *Batrochoglanis*, *Microglanis*, and *Lophiosilurus*, the *cerebellum's* anterior portion is prolonged as far as the boundary between *mesencephalon* and *telencephalon* but does not meet the latter and exhibiting *habenula* in the dorsal portion of the *diencephalon* (state 2).

71. *Lobus facialis*; shape (char. 7): (0) elongated; (1) reduced (Fig. 10) (CI 1.00; RI 1.00). In Ictaluridae, Heptapteridae, and Pimelodidae, the *lobus facialis* is elongated, comprising more than half the length of the lateral-line lobe (state 0). It is the same in several Pseudopimelodidae species, but in *Lophiosilurus*, the *lobus facialis* is reduced, comprising less than half the length of the lateral-line lobe (state 1).

72. *Cerebellum*; shape (char. 8): (0) elongated sagittal, length greater than its width; (1) wide coronal, width greater than its length (CI 1.00; RI 1.00). The *cerebellum* is elongated in all species examined herein, but in *Batrochoglanis* and *Microglanis*, the *cerebellum* is broader as state 1 (Fig. 10).

73. *Cerebellum*; relative volume (char. 9): (0) more voluminous than *telencephalon*; (1) less voluminous than *telencephalon* (Fig. 10) (CI 1.00; RI 1.00). In all examined species, the cerebellum is the broadest subdivision of the brain (state 0). However, in *Batrochoglanis* and *Microglanis*, the *cerebellum* is less voluminous than the *telencephalon* (state 1).

74. Crest on the dorsal surface of the *cerebellum* (char. 10): (0) absent; (1) present (Fig. 10) (CI 1.00; RI 1.00). There is no crest along the *cerebellum's* dorsal surface (state 0) of all examined species, except in *Rhyacoglanis*, where lateral depressions form the crest in the *cerebellum's* parasagittal plane (state 1).

Geometric morphometry character. One character was recovered from geometric morphometry analysis:

75. Shape configuration of the head. Fourteen landmarks of the head of Pseudopimelodidae and outgroups were analyzed (Fig. 3). The set of landmarks from the head forms a configuration that represents one character in the phylogenetic analysis, and the contribution of this configuration is equivalent to that of one discrete character. Each change of position in homologous landmarks represents a different state of this character. The landmarks under parsimony allow visualization of their displacement along the branches (Fig. 11; see Figs. **S3** and **S4**) (CI 0.92; RI 0.83).

Phylogenetic analysis. The combined morphological data parsimony analysis recovered a single most parsimonious tree (Fig. 12), CI = 0.63, and RI = 0.76, with the best score hitting 5000 times out of 5000 resamplings. Pseudopimelodidae was recovered as a monophyletic group and supported by 13 characters. Within Pseudopimelodidae, two lineages were recovered, one composed by (*Rhyacoglanis* (*Cruciglanis*, *Pseudopimelodus*)), with five characters and support of 63%, and the other by (*Lophiosilurus* (*Microglanis*, *Batrochoglanis*)), with nine characters and support of 76%. The characters supporting all the branches are presented in Fig. 12, and the change in character states is in Tab. **S5**.

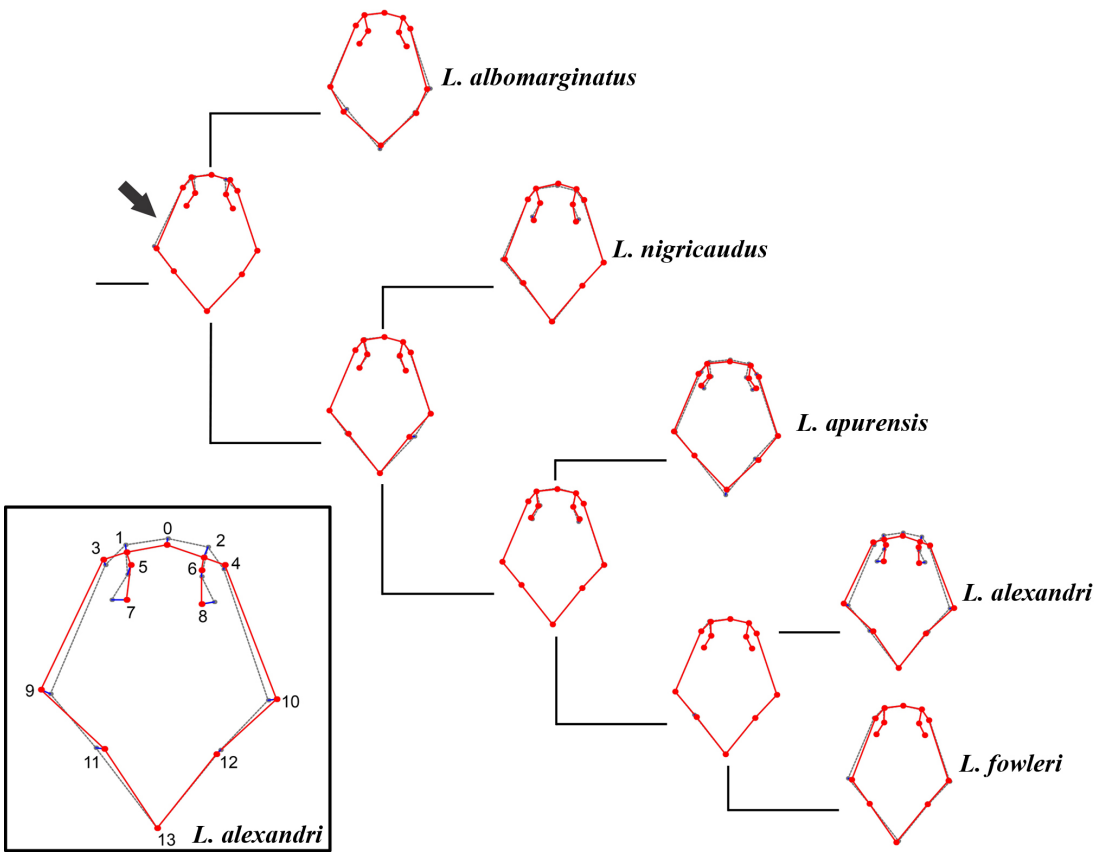

FIGURE 11 | Inferred phylogeny and landmark mapping (numbers) on the head of *Lophiosilurus* species. The arrow indicates the ancestral configuration. Enlarged image of *Lophiosilurus alexandri* in the box (grey lines = ancestral shape; red lines = reconstructed shape, blue lines = landmark position changing to the corresponding node in the ancestor).

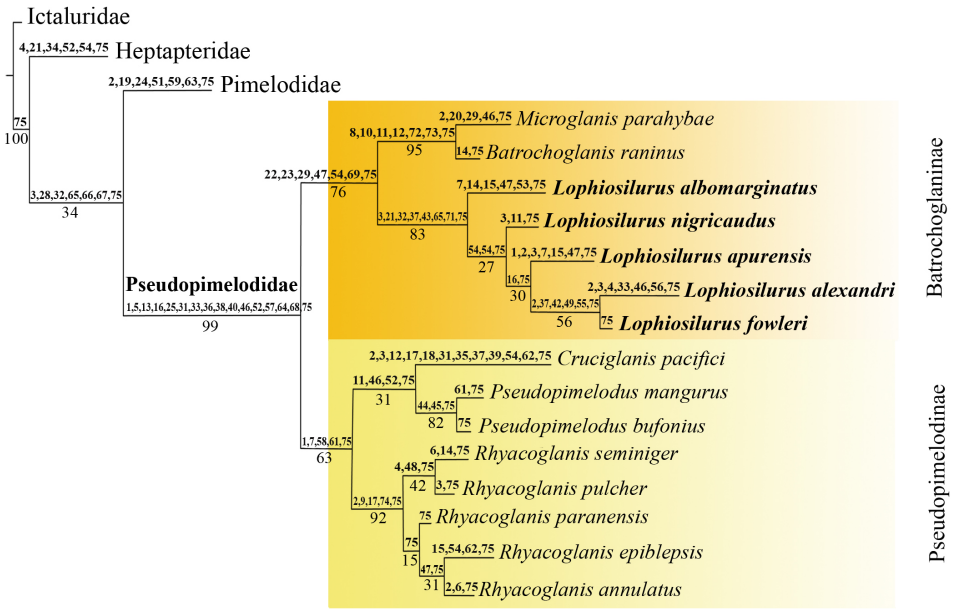

FIGURE 12 | Resampled tree (CI = 63; RI = 76; length (best score) = 148.87) of Pseudopimelodidae derived from combined 75 characters matrix data set, with synapomorphies above and support values (symmetric resampling) under the branches. Pseudopimelodidae subfamilies names according to Silva *et al.* (2021).

Although the wideness of the head can be confirmed with the naked eye, the phylogenetic significance and subtle changes are visualized more easily by geometric morphometry analysis. The change in this species is evidenced by comparing the landmark displacements to the ancestral shape, obtained by applying spatial optimization on the landmarks of each configuration of the head shape. The widening of head shape, easily observed by the lateral displacement of landmarks 9 and 10, shows different states in the family Pseudopimelodidae, reaching the most significant displacement in *Lophiosilurus alexandri* (Fig. 11). Other states of this character (head shape configuration) in the *Lophiosilurus* clade are very subtle to point out, such as the posterior displacement of anterior nostrils (landmarks 1 and 2) and medial displacement of the eyes (landmarks 7 and 8). In *Lophiosilurus apurensis*, the sister species of *L. alexandri* and *L. fowleri*, the eyes are more laterally displaced (landmarks 7 and 8), and the predorsal region is shortened (anterior displacement of landmark 13). The morphology differences in the head of the species based on landmarks are presented in Figs. **S3** and **S4**.

Following the phylogenetic analysis, the morphological characterization of the expanded *Lophiosilurus* genus is:

Lophiosilurus Steindachner, 1876

Lophiosilurus alexandri Steindachner, 1876:154 [106], Pl. 15 (original description).
Pseudopimelodus agassizii Steindachner, 1880:61 (unnecessary name for replacement of *Lophiosilurus alexandri* Steindachner, 1876).
Cephalosilurus Haseman, 1911:317, Pl. (description of *Cephalosilurus fowleri*, the type of the genus).

Diagnosis. The following characters support *Lophiosilurus*: 1) reduction of body depth relative to pectoral girdle width (ch. 3: 65.2–76.9%>63–65%); 2) parieto-supraoccipital trapezoidal, posteriorly expanded (ch. 51: 1>0); 3) posterior portion of entopterygoid with a posterior projection (ch. 56: 0>1); 4) posterior portion of maxillary bone semi-circular (ch. 57: 0>2); 5) gill rakers on first branchial arch bifurcated or even branched (ch. 58: 0>1); 6) intumescence on *lobus facialis* anteriorly placed (ch. 63: 1>2); 7) *lobus facialis* reduced (ch. 69: 0>1); 8) snout shortening, increase in the anterior and posterior nostrils distance, interorbital distance, head width, and shortening of the predorsal region, as observed in the displacement of the landmarks 0, 1, 2, 5, 6, 8, 9, 11, and 13 (ch. 75). Other characters of the genus are: small to large body size, between 116 and 490 mm SL; body depressed; large, angled head at the edges of the mouth; usually prognathous; anterior nostrils located on the upper lips; lateral margin of the premaxillary dentigerous plate projected posteriorly; pectoral-fin spine covered by a thin skin; pectoral fin 6 to 7 branched rays; axillary pore present; pelvic fin starting at vertical through the base of the fourth or of the penultimate branched ray of dorsal fin; caudal fin rounded or with the upper lobe longer; lateral line complete; variable color pattern, with dark subdorsal and subadipose dark brown blotches, irregularly shaped or with only a few spots scattered across the trunk; the color of caudal fin ranging from light brown without dark spots to completely dark brown or black.

Remarks. *Lophiosilurus alexandri* presents the most depressed head and several autapomorphies that kept it a separate genus among Pseudopimelodidae. However, according to the relationship of *Lophiosilurus alexandri*, as shown in Fig. 9, *Cephalosilurus* is a synonym of *Lophiosilurus*. According to the International Code of Zoological Nomenclature (ICZN, 1999; Art. 23), *Lophiosilurus* Steindachner, 1876, prioritizes *Cephalosilurus* Haseman, 1911. Therefore, all species of *Cephalosilurus* must be rearranged accordingly (Tab. 1): *Lophiosilurus albomarginatus* (Eigenmann, 1912), *Lophiosilurus apurensis* (Mees, 1978), *Lophiosilurus fowleri* (Haseman, 1911), and *Lophiosilurus nigricaudus* (Mees, 1974) new combination.

TABLE 1 | Key taxonomic publications with changes in the names of *Lophiosilurus* species. † undescribed fossil species identified by Lundberg *et al.* (2010).

Nominal species	Mees (1974)	Shibatta (2003b)	Current contribution
Cephalosilurus fowleri Haseman, 1911	*Pseudopimelodus fowleri*	*Cephalosilurus fowleri*	*Lophiosilurus fowleri* (Haseman, 1911)
Cf. *Cephalosilurus* sp.†	–	–	*Lophiosilurus* sp.
Lophiosilurus alexandri Steindachner, 1876	–	*Lophsiosilurus alexandri*	*Lophiosilurus alexandri* Steindachner, 1876
Pseudopimelodus albomarginatus Eigenmann, 1912	*Pseudopimelodus albomarginatus*	*Cephalosilurus albomarginatus*	*Lophiosilurus albomarginatus* (Eigenmann, 1912)
Pseudopimelodus apurensis Mees, 1978	–	*Cephalosilurus apurensis*	*Lophiosilurus apurensis* (Mees, 1978)
Pseudopimelodus nigricauda Mees, 1974	*Pseudopimelodus nigricauda*	*Cephalosilurus nigricaudus*	*Lophiosilurus nigricaudus* (Mees, 1974)

The range of distribution of extant species of *Lophiosilurus* includes the São Francisco river basin, Brazil (*L. alexandri* and *L. fowleri*), Orinoco river basin, Venezuela and Colombia (*L. apurensis*), coastal rivers of Guyana (*L. albomarginatus*), and Suriname (*L. nigricaudus*) (Fig. 1). Lundberg *et al.* (2010) identified some dorsal-fin spine fossils from Amazon Neogene as belonging to a species of Pseudopimelodidae. According to the authors, the spines are "robust, with a distinctively short shaft and broad base". Some are from the current Acre river basin in Peru, and others are from the Cuenca basin, Ecuador. The formation where they occur is from the middle-late Miocene. The authors further note that the spines were previously identified as *Pseudopimelodus* (Lundberg, 1998) but could belong to *Cephalosilurus*. The authors' spine photo (Lundberg *et al*., 2010, p. 282) is from a relatively large specimen (we estimated the spine's length from the lateral point of greatest width to the apical extremity = 26 mm). The largest width of the spine is nearly 50% of that length. This proportion is not found in any living species of Pseudopimelodidae (*L. alexandri* (43.4% (n = 1); *L. fowleri* = 42.1% (n = 1); *L. apurensis* = 38.4% (n = 1); *L. albomarginatus* = 36.4–38.7 (n = 2); *Pseudopimelodus mangurus* (36.4–37.2% (n = 2)), but the shape of the spine connects this fossil to *L. fowleri* and *L. alexandri.* Therefore, due to its differences in morphometric proportions, it could be an undescribed species of *Lophiosilurus*. This new species of *Lophiosilurus* from the fossil records expands the distribution range of the genus.

DISCUSSION

Pseudopimelodidae phylogeny. The monophyly of Pseudopimelodidae was highly supported (100%), corroborating previous hypotheses (Lundberg *et al*., 1991a; Shibatta, 1998; Shibatta, 2003b; Ortega-Lara, Lehmann, 2006; Birindelli, Shibatta 2011; Sullivan *et al*., 2013; Shibatta, Vari, 2017; Rangel-Medrano *et al*., 2020; Fig. 2). However, intergeneric relationships were quite variable in all these analyses. Lundberg *et al*. (1991a) and Shibatta (1998; 2003b) recovered *Pseudopimelodus* as the sister group of other genera (Fig. 2A). Ortega-Lara, Lemann (2006) had the *Lophiosilurus* clade as the sister of all other genera (Fig. 2B). Sullivan *et al*. (2013) supported *Batrochoglanis raninus* as the sister group of all other pseudopimelodids (Fig. 2D). The hypotheses published by Shibatta, Vari (2017), and Silva *et al*. (2021) were quite similar but differed in the relationships among *Cruciglanis*, *Pseudopimelodus*, and *Rhyacoglanis* (Figs. 2E, and G). This study corroborates the phylogenetic hypothesis of Pseudopimelodidae genera presented by Shibatta, Vari (2017).

Although they recovered different relationships among genera, all those studies supported a close relationship between *Cephalosilurus* and *Lophiosilurus*. Birindelli, Shibatta (2011) was the first to include almost all species of *Lophiosilurus* in the phylogenetic analysis (Fig. 2C) and observed that *L. apurensis*, *L. fowleri*, *L. nigricaudus*, and *L. alexandri* were unique among pseudopimelodids by possessing the constrictor muscle of the gas bladder. The absence of the constrictor muscle in *L. albomarginatus* was the main character to point out the polyphyly of the *Cephalosilurus*. However, according to our present analysis, the absence of the gas bladder muscle is a plesiomorphy.

This contribution points to the evolution of two clades within Pseudopimelodidae, each with strong support (77 and 61%). A different relationship within

Pseudopimelodidae was found in a previous study by Sullivan *et al*. (2013; Fig. 2D). The authors analyzed five species of four genera of Pseudopimelodidae in a study on the phylogeny of the Pimelodoidea superfamily, using rag1 and rag2 nuclear and 12S and 16S rDNA mitochondrial genes. The hypothesis of *Batrochoglanis raninus* as sister to the clade ((*Pseudopimelodus mangurus*, *P. bufonius*), (*Lophiosilurus alexandri*, *Cephalosilurus apurensis*)) was strongly supported both in parsimony and Bayesian analysis. However, the incomplete taxon sampling (*Microglanis*, *Rhyacoglanis*, and *Cruciglanis* were missing) may have impaired the consistency of these relationships. More recently, Rangel-Medrano *et al*. (2020) examined the mitochondrial cox1 (or COI) and nuclear rag2 genes, including *Cruciglanis*, *Microglanis*, and *Rhyacoglanis* in the analysis, and presented a phylogenetic tree that corroborates the two lineages evidenced by Shibatta, Vari (2017). According to the dated phylogeny of those authors, these lineages may have diverged in the upper Eocene, just under 40 mya. Both lineages were recently recovered by Silva *et al.* (2021) using nuclear loci of ultraconserved elements analysis. Silva *et al*. (2021) recognized one of the clades as subfamily Pseudopimelodinae and described the other as subfamily Batrochoglaninae.

Geometric morphometry and evolution of head shape in Pseudopimelodidae. In this study, the geometric morphometric character had low homoplasy levels and can be interpreted as phylogenetically informative. The results of the present study clearly show that landmark data can be an important source of evidence for phylogenetic analysis. The analysis of morphological data also provides a potential source of alternative evidence that can be used to complement other data. Phylogenetic morphological studies generate a vast amount of biological knowledge presented in a systematized and ordered manner, representing relevant data for systematists (Catalano *et al*., 2015).

The head shape configuration had high values of consistency and retention indices. Although morphometry is widely explored in taxonomy, it has only recently been used in phylogenetic analyses (Adams *et al*., 2004; Gonzalez-José *et al*., 2008; Klingenberg, Gidaszewski, 2010; Catalano, Torres, 2017; Ospina-Garcés, Luna, 2017). The mapping of different states (changes in the landmark positions) with geometric morphometry (GM) along the branches provided a new evidence source. In addition, this is the first time a landmark data configuration has been combined with other kinds of characters to study Neotropical freshwater fish systematics. Solis-Zurita *et al.* (2019) recommend that morphometric characters be combined with different characters to infer homology and phylogenetic groups. Several authors have noted the advantages of including GM in phylogenetic inferences (David, Laurin, 1996; Larson, 2005; Gonzalez-José *et al*., 2008; Catalano *et al*., 2015; Catalano, Torres, 2017; Ospina-Garcés, Luna, 2017).

The phylogenetic analysis using geometric morphometry helped support the Pimelodoidea clade, an essential contribution to the phylogeny proposed by Shibatta, Vari (2017), who found no synapomorphy for that clade. Using the geometric morphometric character resulted in a wholly solved phylogeny in the *Rhyacoglanis* clade. A small phylogenetic change was observed in *Rhyacoglanis paranensis*, compared to the hypothesis proposed by Shibatta, Vari (2017). In that study, *R. paranensis* was found to be the sister group of all other congeners, while in the current hypothesis, the species is the sister of *R. epiblepsis* and *R. annulatus*. However, studies on the *Rhyacoglanis* species from the Amazon basin are lacking, and the possible inclusion of new species

may alter the configuration of currently known phylogenetic relationships.

A global analysis of landmark positions helped reveal subtle changes which are challenging to see by direct observation of specimens. Furthermore, it was not necessary to create discrete categories with arbitrary limits to demonstrate the variation in the shape of the heads of the studied species. This new data source enables valuable information on the species' shape (Adams *et al*., 2004; Klingenberg, Gidaszewski, 2010). The shape is one of the most important and easily measured phenotype elements and expresses the interaction of many, if not most, genes (Ollier *et al*., 2006; Covain *et al*., 2008).

All *Cephalosilurus* species inclusion allowed testing the genus monophyly and their reallocation into *Lophiosilurus*. A better understanding of the *Lophiosilurus* species morphology allowed us to recognize a new fossil species representing an extinct species that occurred in the Amazon basin, filling an essential geographical gap in the genus's distribution. Using continuous characters instead of discretizing them allowed us to better understand the group's evolution without creating subjective categories. The congruence between the phylogenetic relationships of the Pseudopimelodidae genera obtained with the exclusive use of morphological characters and those obtained by other authors through molecular characters shows the information power of both types of data.

ACKNOWLEDGMENTS

We thank José Luis O. Birindelli for valuable suggestions to improve the manuscript. To the II International Symposium's scientific committee on Phylogeny and Classification of Neotropical Fishes for their invitation to present part of this study at the event. We also thank Scott Shaefer (AMNH), John Lundberg, Mark Sabaj (ANSP), Lucia R. Py Daniel (INPA), Flavio Bockmann (LIRP), Mary Burridge (ROM), Marcelo de Britto (MNRJ), Mario de Pinna, Alex Datovo (MZUSP), and Richard Vari (USNM), for the loan of specimens. Programa de Pós-Graduação em Ciências Biológicas da Universidade Estadual de Londrina and Coordenadoria de Aperfeiçoamento de Pessoal de Nível Superior (CAPES) for supporting LRJ's thesis. Santiago Catalano and Sandra Ospina-Garcés assisted us in the use of TNT for landmark data analysis. This study was partially financed by a grant from the All Catfish Species Inventory (NSF DEB–0315963) and Conselho Nacional de Desenvolvimento Científico e Tecnológico (CNPq; proc. 200280/2014–7). CNPq research productivity grant to OAS (303685/2018–2). VPA was supported by CAPES (grant# 88887.318624/2019–00) and FAPESP (proc. 2014/11397–1; 2015/26804–4; 2016/19075–9; 2017/17957–7). To Maria Luisa Sarmento Soares and Brian Sidlauskas for the manuscript revision.

REFERENCES

- **Abrahão VP, Pupo FM, Shibatta OA.** Comparative brain gross morphology of the Neotropical catfish family Pseudopimelodidae (Osteichthyes, Ostariophysi, Siluriformes), with phylogenetic implications. Zool J Linn Soc. 2018; 184(3):750–72. https://doi.org/10.1093/zoolinnean/zly011
- **Adams DC, Rohlf FJ, Slice DE.** Geometric morphometrics: ten years of progress following the "revolution". Ital J Zool. 2004; 71(1):5–16. https://doi.org/10.1080/11250000409356545

- **Alcaraz HSV, Graça WJ, Shibatta OA.** *Microglanis carlae*, a new species of bumblebee catfish (Siluriformes: Pseudopimelodidae) from the río Paraguay basin in Paraguay. Neotrop Ichthyol. 2008; 6(3):425–32. https://doi.org/10.1590/S1679-62252008000300016
- **Arratia G.** Catfish head skeleton – an overview. In: Arratia G, Kapoor BG, Chardon M, Diogo R, editors. Catfishes. Enfield, England: Science Publishers; 2003a. p.3–46.
- **Arratia G.** The siluriform postcranial skeleton – an overview. In: Arratia G, Kapoor BG, Chardon M, Diogo R, editors. Catfishes. Enfield, England: Science Publishers; 2003b. p.121–57.
- **Assega FM, Birindelli JLO, Bialetzki A, Shibatta OA.** External morphology of *Lophiosilurus alexandri* Steindachner, 1876 during early stages of development, and its implications for the evolution of Pseudopimelodidae (Siluriformes). PloS ONE. 2016; 11:e0153123. https://doi.org/10.1371/journal.pone.0153123
- **Birindelli JLO.** Phylogenetic relationships of the South American Doradoidea (Ostariophysi: Siluriformes). Neotrop Ichthyol. 2014; 12(3):451–564. http://dx.doi.org/10.1590/1982-0224-20120027
- **Birindelli JLO, Shibatta OA.** Morphology of the gas bladder in bumblebee catfishes (Siluriformes, Pseudopimelodidae). J Morphol. 2011; 272(7):890–96. https://doi.org/10.1002/jmor.10961
- **Catalano SA, Ercoli M, Prevosti F.** The more, the better: The use of multiple landmark configurations to solve the phylogenetic relationships in Musteloids. Syst Biol. 2015; 64(2):294–306. https://doi.org/10.1093/sysbio/syu107
- **Catalano SA, Goloboff PA, Giannini NP.** Phylogenetic morphometrics (I): the use of landmark data in a phylogenetic framework. Cladistics. 2010; 26(5):539–49. https://doi.org/10.1111/j.1096-0031.2010.00302.x
- **Catalano SA, Goloboff PA.** Simultaneously mapping and superimposing landmark configurations with parsimony as optimality criterion. Syst Biol. 2012; 61(3):392–400. https://doi.org/10.1093/sysbio/syr119
- **Catalano AS, Goloboff PA.** A guide for the analysis of continuous and landmark characters in TNT (Tree Analysis using New Technologies). Technical Report; 2018. https://doi.org/10.13140/RG.2.2.23797.27360
- **Catalano SA, Torres A.** Phylogenetic inference based on landmark data in 41 empirical datasets. Zool Scr. 2017; 46(1):1–11. https://doi.org/10.1111/zsc.12186
- **Chang I.** Breeding success with the Pac-man catfish, *Lophiosilurus alexandri*. Amazonas. 2013; 2:74–78.
- **Covain RS, Dray S, Fisch-Muller S, Montoya-Burgos JI.** Assessing phylogenetic dependence of morphological traits using co-inertia prior to investigate character evolution in Loricariinae catfishes. Mol Phylogenet Evol. 2008; 46(3):986–1002. https://doi.org/10.1016/j.ympev.2007.12.015
- **David B, Laurin B.** Morphometrics and cladistics: measuring phylogeny in the sea urchin *Echinocardium*. Evolution. 1996; 50(1):348–59. https://doi.org/10.1111/j.1558-5646.1996.tb04498.x
- **Diogo R, Chardon M, Vanderwalle P.** Osteology and myology of the cephalic region and pectoral girdle of *Batrochoglanis raninus*, with a discussion on the synapomorphies and phylogenetic relationship of the Pseudopimelodinae and Pimelodidae (Teleostei: Siluriformes). Anim Biol. 2004; 54(3):262–80. http://hdl.handle.net/2268/246296
- **Farris J.** Methods for computing Wagner trees. Syst Biol. 1970; 19(1):83–92. https://doi.org/10.1093/sysbio/19.1.83
- **Ferrer J, Wingert JM, Malabarba LR.** Description of a new species and phylogenetic analysis of the subtribe Cynopoecilina, including continuous characters without discretization (Cyprinodontiformes: Rivulidae). Zool J Linn Soc. 2014; 172(4):846–66. https://doi.org/10.1111/zoj.12190
- **Fricke R, Eschmeyer WN, Van der Laan R, editors.** Eschmeyer's catalog of fishes: genera, species, references. Available from: http://researcharchive.calacademy.org/research/ichthyology/catalog/fishcatmain.asp. Accessed 04 Nov 2021.
- **Goloboff PA.** Tree searches under Sankoff parsimony. Cladistics. 1998; 14(3):229–37. https://doi.org/10.1006/clad.1998.0068

- **Goloboff PA, Catalano SA.** Phylogenetic morphometrics (II): algorithms for landmark optimization. Cladistics. 2011; 27(1):42–51. https://doi.org/10.1111/j.1096-0031.2010.00318.x
- **Goloboff PA, Catalano SA.** TNT version 1.5, including a full implementation of phylogenetic morphometrics. Cladistics. 2016; 32(3):221–38. https://doi.org/10.1111/cla.12160
- **Goloboff PA, Farris JS, Källersjö M, Oxelman B, Szumik CA.** Improvements to resampling measures of group support. Cladistics. 2003; 19(4):324–32. https://doi.org/10.1111/j.1096-0031.2003.tb00376.x
- **Goloboff PA, Farris JS, Nixon KC.** TNT, a free program for phylogenetic analysis. Cladistics. 2008; 24(5):774–86. https://doi.org/10.1111/j.1096-0031.2008.00217.x
- **Goloboff PA, Mattoni CI, Quinteros AS.** Continuous characters analyzed as such. Cladistics. 2006; 22(6):589–601. https://doi.org/10.1111/j.1096-0031.2006.00122.x
- **González-José R, Escapa I, Neves WA, Cúneo R, Pucciarelli HM.** Cladistic analysis of continuous modularized traits provides phylogenetic signals in *Homo* evolution. Nature. 2008; 453:775. https://doi.org/10.1038/nature06891
- **Gower JC.** Generalized Procrustes analysis. Psychometrika. 1975; 40:33–51. https://doi.org/10.1007/BF02291478
- **Haseman JD.** Descriptions of some new species of fishes and miscellaneous notes on others obtained during the expedition of the Carnegie Museum to central South America. Ann Carnegie Mus. 1911; 7:315–28, pls. 46–52.
- **International Code of Zoological Nomenclature (ICZN).** The International Trust for Zoological Nomenclature, London; 1999. Available from: https://www.iczn.org/the-code/the-international-code-of-zoological-nomenclature/the-code-online.
- **Jarduli LR, Shibatta OA.** Description of a new species of *Microglanis* (Siluriformes: Pseudopimelodidae) from the Amazon basin, Amazonas State, Brazil. Neotrop Ichthyol. 2013; 11(3):507–12. https://doi.org/10.1590/S1679-62252013000300004
- **Klingenberg P, Gidaszewski NA.** Testing and quantifying phylogenetic signals and homoplasy in morphometric data. Syst Biol. 2010; 59(3):245–61. https://doi.org/10.1093/sysbio/syp106
- **Larson PM.** Ontogeny, phylogeny, and morphology in anuran larvae: morphometric analysis of cranial development and evolution in *Rana* tadpoles (Anura: Ranidae). J Morphol. 2005; 264(1):34–52. https://doi.org/10.1002/jmor.10313
- **Lundberg JG, Berra TM, Friel JP.** First description of small juveniles of the primitive catfish *Diplomystes* (Siluriformes: Diplomystidae). Ichthyol Explor Freshw. 2004; 15(1):71–82. Available from: https://mansfield.osu.edu/assets/mansfield/tberra/pdf/Diplomystes.pdf
- **Lundberg JG, Bornbusch AH, Mago-Leccia F.** *Gladioglanis conquistador* n. sp. from Ecuador with diagnoses of the subfamilies Rhamdiinae Bleeker and Pseudopimelodinae n. subf. (Siluriformes: Pimelodidae). Copeia. 1991a; 1991(1):190–209. https://doi.org/10.2307/1446263
- **Lundberg JG, Mago-Leccia F, Nass P.** *Exallodontus aguanai*, a new genus and species of Pimelodidae (Pisces: Siluriformes) from deep river channels of South America and delimitation of the subfamily Pimelodinae. Proc Biol Soc Wash. 1991b; 104(4):840–69.
- **Lundberg JG, Sabaj MH, Dahdul WM, Aguilera OA.** The Amazonian Neogene fish fauna. In: Hoorn C, Wesselingh FP, editors. Amazônia: Landscape and species evolution: A look into de past. Hoboken, NY: Blackwell Publishing Ltd.; 2010. p.281–301.
- **Mees GF.** The Auchenipteridae and Pimelodidae of Suriname (Pisces, Nematognathi). Zoolog Verh (Leiden). 1974; 132:1–256. Available from: https://repository.naturalis.nl/pub/317592
- **Ollier S, Couteron P, Chessel D.** Orthonormal transform to decompose the variance of a life-history trait across a phylogenetic tree. Biometrics. 2006; 62(2):471–77. https://doi.org/10.1111/j.1541-0420.2005.00497.x
- **Ortega-Lara A, Lehmann PA.** *Cruciglanis*, a new genus of Pseudopimelodid catfish (Ostariophysi: Siluriformes) with description of a new species from the Colombian Pacific coast. Neotrop Ichthyol. 2006; 4(2):147–56. https://doi.org/10.1590/S1679-62252006000200002

- **Ospina-Garcés SM, Luna ED.** Phylogenetic analysis of landmark data and the morphological evolution of cranial shape and diets in species of *Myotis* (Chiroptera: Vespertilionidae). Zoomorphology. 2017; 136:251–65. https://doi.org/10.1007/s00435-017-0345-z
- **Rangel-Medrano J, Ortega-Lara A, Márquez EJ.** Ancient genetic divergence in bumblebee catfish genus *Pseudopimelodus* (Pseudopimelodidae: Siluriformes) from northwestern South America. PeerJ. 2020; 8:e9028. http://doi.org/10.7717/peerj.9028
- **Rohlf FJ.** *tpsDig v.2.21*. Distributed by the author, Department of Ecology and Evolution. New York: State University of New York, Stony Brook; 2015.
- **Rohlf FJ.** *tpsRelw v.1.65*. Distributed by the author, Department of Ecology and Evolution. New York: State University of New York, Stony Brook; 2016.
- **Rohlf FJ, Slice D.** Extensions of the Procrustes method for the optimal superimposition of landmarks. Syst Zool. 1990; 39(1):40–59. https://doi.org/10.2307/2992207
- **Ruiz WBG, Shibatta OAS.** A new species of *Microglanis* (Siluriformes, Pseudopimelodidae) from lower rio Tocantins basin, Pará, Brazil, with description of superficial neuromasts and pores of lateral line system. Zootaxa. 2010; 2632:53–66. https://doi.org/10.11646/zootaxa.2632.1.3
- **Sabaj MH.** Standard symbolic codes for institutional resource collections in herpetology and ichthyology: an online reference. Version 7.1; 2019. Available from: https://asih.org/standard-symbolic-codes/about-symbolic-codes
- **Sankoff D, Rousseau P.** Locating the vertices of a Steiner tree in an arbitrary space. Math Program. 1975; 9:240–46. https://doi.org/10.1007/BF01681346
- **Solis-Zurita C, De Luna E, González D.** Phylogenetic relationships in the *Sceloporus variabilis* (Squamata: Phrynosomatidae) complex based on three molecular markers, continuous characters and geometric morphometric data. Zool Scr. 2019; 48(4):419–39. https://doi.org/10.1111/zsc.12349
- **Santos HB, Sampaio EV, Arantes FP, Sato Y.** Induced spawning and reproductive variables of the catfish *Lophiosilurus alexandri* Steindachner, 1876 (Siluriformes: Pseudopimelodidae). Neotrop Ichthyol. 2013; 11(3):607–14. https://doi.org/10.1590/S1679-62252013000300014
- **Shibatta OA.** Sistemática e evolução da família Pseudopimelodidae (Ostariophysi, Siluriformes), com a revisão taxonômica do gênero *Pseudopimelodus*.[PhD Thesis]. São Carlos: Universidade Federal de São Carlos; 1998.
- **Shibatta OA.** Phylogeny and classification of 'Pimelodidae'. In: Arratia G, Kapoor BG, Chardon M, Diogo R, editors. Catfishes. Enfield, England: Science Publishers; 2003a. p.385–400.
- **Shibatta OA.** Family Pseudopimelodidae (Bumblebee catfishes, dwarf marbled catfishes). In: Reis RE, Kullander SO, Ferraris Jr CJ, organizers. Check List of the Freshwater Fishes of South and Central America Porto Alegre: Edipucrs; 2003b. p.401–405.
- **Shibatta AO, Benine RC.** A new species of *Microglanis* (Siluriformes: Pseudopimelodidae) from upper rio Paraná basin, Brazil. Neotrop Ichthyol. 2005; 3(4):579–85. https://doi.org/10.1590/S1679-62252005000400015
- **Shibatta OA, Pavanelli CS.** Description of a new *Batrochoglanis* species (Siluriformes, Pseudopimelodidae) from the rio Paraguai basin, State of Mato Grosso, Brazil. Zootaxa. 2005; 1092(1):21–30. https://doi.org/10.11646/zootaxa.1092.1.2
- **Shibatta OA.** A new species of *Microglanis* (Siluriformes: Pseudopimelodidae) from the upper rio Tocantins basin, Goiás State, Central Brazil. Neotrop Ichthyol. 2014; 12(1):81–87. https://doi.org/10.1590/S1679-62252014000100008
- **Shibatta OA.** New species of bumblebee catfish of the genus *Batrochoglanis* Gill, 1858 (Siluriformes: Pseudopimelodidae) from the Aripuanã river basin, Mato Grosso, Brazil. Zootaxa, 2019; 4674(2):243–63. https://doi.org/10.11646/zootaxa.4674.2.6
- **Shibatta OA, van der Sleen P.** Family Pseudopimelodidae-bumblebee catfishes, dwarf-marbled catfishes. In: van der Sleen P, Albert J, editors. Field Guide to the fishes of the Amazon, Orinoco & Guianas New Jersey: Princeton University Press; 2018. p.308–10.

- **Shibatta OA, Vari RP.** A new genus of Neotropical rheophilic catfishes, with four new species (Teleostei: Siluriformes: Pseudopimelodidae). Neotrop Ichthyol. 2017; 15(2):e160132. https://doi.org/10.1590/1982-0224-20160132
- **Silva GSC, Melo B, Roxo FF, Ochoa LE, Shibatta OA, Sabaj MH, Oliveira C.** Phylogenomics of the bumblebee catfishes (Siluriformes: Pseudopimelodidae) using ultraconserved elements. Jour Zool Syst Evol Res. Forthcoming 2021. http://doi.org/10.1111/jzs.12513
- **Steindachner F.** Ichthyologische Beiträge (V). [Subtitles i-v.]. Sitzungsberichte der Kaiserlichen Akademie der Wissenschaften. Math Naturwiss Kl. 1876; 74:49–240, pls. 1–15.
- **Steindachner F.** Zur Fisch-Fauna des Cauca und der Flüsse bei Guayaquil. Denkschriften der Kaiserlichen Akademie der Wissenschaften in Wien, Math Naturwiss Kl. 1880; 42:55–104, pls. 1–9.
- **Sullivan JP, Muriel-Cunha J, Lundberg JG.** Phylogenetic relationships and molecular dating of the major groups of catfishes of the Neotropical superfamily Pimelodoidea (Teleostei, Siluriformes). P Acad Nat Sci Phila. 2013; 162:89–110. https://www.jstor.org/stable/42751950

AUTHORS' CONTRIBUTION

Oscar Akio Shibatta: Conceptualization, Data curation, Formal analysis, Funding acquisition, Investigation, Methodology, Project administration, Resources, Supervision, Validation, Visualization, Writing-original draft, Writing-review and editing.

Lucas Ribeiro Jarduli: Conceptualization, Data curation, Formal analysis, Investigation, Methodology, Validation, Visualization, Writing-original draft, Writing-review and editing.

Vitor Pimenta Abrahão: Conceptualization, Data curation, Formal analysis, Investigation, Methodology, Validation, Visualization, Writing-original draft, Writing-review and editing.

Lenice Souza-Shibatta: Conceptualization, Formal analysis, Investigation, Methodology, Validation, Visualization, Writing-original draft, Writing-review and editing.

ETHICAL STATEMENT

Specimens examined in this study were available in collections.

COMPETING INTEREST

The authors declare no competing interest

HOW TO CITE THIS ARTICLE

- **Shibatta OA, Jarduli LR, Abrahão VP, Souza-Shibatta L.** Phylogeny of the Neotropical Pacman catfish genus *Lophiosilurus* (Siluriformes: Pseudopimelodidae). Neotrop Ichthyol. 2021; 19(4):e210040. https://doi.org/10.1590/1982-0224-2021-0040

Neotropical Ichthyology

OPEN ACCESS

SBI Official Journal of the Sociedade Brasileira de Ictiologia